Atomic Population of Effectively Localized Electrons of Polycyclic Aromatic Hydrocarbons with the KP16/B13 Density Functional

by

Dwayne John

A dissertation submitted in partial fulfilment of the requirements of the degree of Doctor of Philosophy in Computational Science

Middle Tennessee State University
May 2021

Dissertation Committee:
Jing Kong, Chair
Tibor Koritszansky
Henrique Momm
Don Ye
John Wallin

Dedication

To all of those who helped in this journey along the way. You know who you are!

Acknowledgements

I would first like to thank my advisor Dr. Jing Kong. We both started at MTSU at the same time in Fall of 2013 and it has been an interesting and fulfilling journey to say the least. Not many advisors would take on a non-traditional graduate student but Dr. Kong did not hesitate in the slightest to take me under his wing.

I would also like to thank Dr. Wallin. It was his initial foresight that put Dr. Kong and I together.

Special thanks to Emil Proynov, Jianguo, and Fenglai Liu.

Thank you to my fellow graduate students Matthew Wang and Conrad Lewis.

ABSTRACT

Polycyclic aromatic hydrocarbons, also known as PAHs, have been studied by scientists for over a century. Besides their large volume and low molecular weight, presentations of past findings show that most neutral ground state PAHs possess a closed-shell electronic configuration. Several years ago, newer studies showed that some polycyclic hydrocarbons could have a singlet biradical ground state, showing new, and possibly ground-breaking optical and magnetic properties. If these molecules are proven to be stabilized, this could lead to more applicable organic electronics, nonlinear optics, organic spintronics and photovoltaics, and energy storage devices. Obtaining a physics description using quantum chemistry methods would also be advantageous to the study of the properties of industrial molecules.

In this work, various spin multiplicities of structures of polycyclic hydrocarbons are studied using the quantum chemistry method known as Atomic Population of Effectively Localized Electrons (APELE), with the KP16/B13 functional. Bond length and potential energy calculations of theoretical diatomic carbon were also investigated. Results indicate that there is validity in future applications of these systems using the method of APELE [66].

The strongly constrained and appropriately normed (SCAN) semilocal density functional was also implemented in Fortran to calculate several noble gases. Calculations were used to make better adjustments to the Kong-Proynov16/Becke13 DFT.

TABLE OF CONTENTS

List of Figures

List of Tables

1 INTRODUCTION

> "Quantum physics forms the foundation of chemistry, explaining how molecules are held together. It describes how real solids and materials behave and how electricity is conducted through them... It enabled the development of transistors, integrated circuits, lasers, LEDs, digital cameras and all the modern gadgetry that surrounds us." -Neil Turok

1.1 Quantum Chemistry

What is Quantum Chemistry? In essence, we are asking the question: what is a molecule? Quantum chemistry, also referred to as molecular quantum mechanics, seeks to answer the questions focused on the application of quantum mechanics in physical models and chemical systems.

Energy is the main physical property studied in Quantum Chemistry and Quantum Chemistry is the art of approximation in solving partial differential equations. At the heart of computational chemistry is the mathematical manipulation of matrices: eigenvectors and eigenvalues, therefore it is not surprising that a majority of calculations in Quantum Chemistry involve solving symmetric, real, matrices, so the focus is on manipulating and computing them.

1.1.1 Quantum Mechanics

Quantum Mechanics is the foundation of Quantum Chemistry. Quantum Mechanics is made of formulas that are tools for solving problems involving microscopic systems, in which there are two representations: a Matrix and a Function. By implementing and using these tools, one has no choice but to think differently about the universe[48] as opposed to the more traditional classical understanding.

1.1.2 Postulates of Quantum Mechanics

There are six postulates of Quantum Mechanics. A postulate in essence is the assumption or suggestion of something as true based on reasoning, discussion, or belief. The first postulate states that "every physically-realizable state of a system is described in quantum mechanics by a state function, Ψ, that contains all accessible physical information about the system in that state[48]."

The second postulate of Quantum Mechanics says that "If a system is in a quantum state represented by a wave function Ψ, then $Pdv = |\Psi|^2 dv$ is the probability that in a position measurement at time t the particle will be detected in the infinitesimal volume element dv," analogous to the laws of statistics. The wave function expressed in this way, $\Psi = \Psi(position, time)$, show that in quantum physics, position and time are independent quantities[48]." So for every observable quantity in classical physics exists a linear Hermitian quantum operator.

The Principle of Superposition says that "If Ψ_1 and Ψ_2 represent two physically-realizable states of a system, then the linear combination $\Psi = c_1\Psi_1 + c_2\Psi_2$, where c_1 and c_2 are arbitrary complex constants, represents a third physically-realizable state of the system." This is more formally stated in the fourth postulate.

The third postulate of Quantum Mechanics says that observables are characterized by operators, or an instruction represented by a symbol which tells you to do a mathematical act on a function. The operator finds physical values about the observable from state functions. The quantum representation of an observable in classical physics, Q(x,p) is operator $\hat{Q}(\hat{x}, \hat{p})$.

The fourth postulate of Quantum Mechanics defines the quantum average value of an observable.

The fifth postulate states that the wavefunction develops gradually in time via the time-dependent Schrödinger equation $i\hbar\frac{\partial}{\partial t}\Psi(\mathbf{r}, t) = \hat{H}\Psi(\mathbf{r}, t)$.

The sixth postulate of Quantum Mechanics says that the total wavefunction has to be antisymmetric with respect to the interchange of all coordinate locations of one fermion in relation to the others. The quantity spin has to be included in the coordinates.

Before arriving at Schrödinger's Equation, it is necessary to consider that it can be formed from the classical wave equation, which in turn can be derived from Maxwell's equations given below

$$\nabla \cdot \vec{E} = \frac{\rho}{\epsilon_0} \tag{1}$$

$$\nabla \cdot \vec{B} = 0 \tag{2}$$

$$\nabla \times \vec{E} = -\frac{\partial \vec{B}}{\partial t} \tag{3}$$

$$\nabla \times \vec{B} = \mu_0 \vec{J} + \mu_0 \epsilon_0 \frac{\partial \vec{E}}{\partial t} \tag{4}$$

Use the left sides of equation 1.3 and equation 1.1 and act on them with their respective operators while setting them equal to each other[25].

$$\nabla \times (\nabla \times \vec{E}) = \nabla \cdot (\nabla \cdot \vec{E}) - \nabla^2 \vec{E} \tag{5}$$

$$\nabla \times (\nabla \times \vec{E}) = -\nabla^2 \vec{E} \tag{6}$$

$$\nabla \times \left(-\frac{\partial \vec{B}}{\partial t} \right) = -\nabla^2 \vec{E} \tag{7}$$

$$-\frac{\partial}{\partial t} \left(\nabla \times \vec{B} \right) = -\nabla^2 \vec{E} \tag{8}$$

$$\tag{9}$$

Replace $\nabla \times \vec{B}$ using the right side of equation 1.4 which yields

$$-\frac{\partial}{\partial t}\left(\mu_0 \vec{J} + \mu_0 \epsilon_0 \frac{\partial \vec{E}}{\partial t}\right) = -\nabla^2 \vec{E} \tag{10}$$

Set $\nabla \cdot \vec{E}$ equal to zero since the charge density ρ is zero in free space. There is no current density.

Again, we are saying there is no current density in free space, therefore $\vec{J} = 0$, so we now get.

$$\frac{1}{c^2}\left(-\frac{\partial^2 E}{\partial t^2}\right) = -\nabla^2 \vec{E} \tag{11}$$

The above partial differential equation, also known as the wave equation, can be solved using separation of variables using the following solution

$$E(r,t) = \Psi(x) cos(\omega t) \tag{12}$$

In the above equation, E is the electric field.

The evolution of the system is described by the Schrödinger equation. Since the Schrödinger equation is also a partial differential equation, like the one above which was derived from Maxwell's equations, we can leverage that notion into constructing a similar one for ourselves. It will be a general solution to the Schrödinger equation.

We call this solution the wave function and it is denoted by Ψ, with the simplest wave function being written in plane wave form.

$$\Psi(r,t) = Ae^{i(k \cdot r - \omega t)} \tag{13}$$

The amplitude is A, wave vector k, ω angular frequency of the plane wave. These plane waves are combined using the superposition principle to create a linear combination of them that can then be used in the Schrödinger equation once the necessary transformations are made: momentum, energy, space, time, etc.

"The wave function Ψ governs the motion of the electrons in the same way as light waves determine the motion of the photons - wherever Ψ vanishes there are no electrons.[31]"

The general simple form of the Schrödinger equation is written as the following.

$$\hat{H}\Psi = \hat{E}\Psi \tag{14}$$

Where $\hat{H}$ is the Hamiltonian operator, Ψ is the wavefunction, and $\hat{E}$ is the energy, not to be confused with the electric field earlier. The general equation can be cast into two different forms, the time-dependent and time-independent Schrödinger equation shown below.

$$\hat{H}\Psi = i\hbar\frac{\partial\Psi}{\partial t} \tag{15}$$

$$\hat{H}\Psi = E\Psi \tag{16}$$

The first equation includes the partial derivative with respect to time, denoting it as the time-dependent Schrödinger equation. For the time-independent equation, energy no longer changes over time. For the purposes of this work, the focus is the time-independent Schrödinger equation due to the state of the atomic or molecular system remaining constant over time.

1.2 Introduction to Density Functional Theory

Density Functional Theory (DFT) was used by condensed matter physicists long before it was picked up by chemists[14].

In DFT, we are solving the time independent Schrödinger Equation in 3-space. Because of the Uncertainty Principle, the time range Δt=10^{-6}s to 10^{10}s is very long in the quantum realm, we can approximate that the time is zero. The uncertainty range for energy is ΔE= 3.31×10^{-24}J to 3.31×10^{-28}J. The key point here is that time doesn't effect the measurement so it can be removed from being involved in our calculations, thus temporarily ignoring the first Axiom of Quantum Mechanics.

We start with the molecular Hamiltonian which gives us the total energy of the molecular system.

$$\hat{H} = \hat{T}_n + \hat{T}_e + \hat{U}_{e-n} + \hat{U}_{e-e} + \hat{U}_{n-n} \tag{17}$$

Electronic KE (single electron),

$$\hat{T}_e = -\sum_i \frac{\nabla_i^2}{2} \tag{18}$$

Electronic PE (electron-nucleon interaction),

$$\hat{U}_{e-n} = -\sum_{i,I} \frac{Z_I}{|R_I - \hat{r}_i|} \tag{19}$$

Electronic PE (electron-electron interaction),

$$\hat{U}_{e-e} = -\sum_{i \neq j} \frac{1}{|\hat{r}_i - \hat{r}_j|} \tag{20}$$

Nuclear PE, (nucleon-nucleon interaction)

$$\hat{U}_{e-n} = -\sum_{I \neq J} \frac{Z_I Z_J}{|R_I - R_J|} \tag{21}$$

$$\hat{H} = -\sum_{i=1}^{N} \frac{1}{2}\nabla_i^2 - \sum_{A=1}^{M} \frac{1}{2M_A}\nabla_A^2 - \sum_{i=1}^{N}\sum_{A=1}^{M} \frac{Z_A}{r_{iA}} + \sum_{i=1}^{N}\sum_{j>i}^{N} \frac{1}{r_{ij}} + \sum_{A=1}^{M}\sum_{B>A}^{M} \frac{Z_A Z_B}{R_{AB}} \tag{22}$$

"The terms are as follows: N is the number of electrons, M is the number of nuclei, M_A is the ratio of the mass of nucleus A to the mass of an electron, Z_A is the atomic number of nucleus A, r_{iA} is the distance between nucleus A and electron i, r_{ij} is the distance between electron i and j, and R_{AB} is the distance between nucleus A and nucleus B. The differentiation operators ∇_i^2 and ∇_A^2 are with respect to the coordinates of the ith electron and Ath nucleus respectively. The first and second terms of the Hamiltonian are the kinetic energy operators for the electrons and nuclei respectively. The third term is the Coulomb attraction between electron i and nucleus A. The fourth term is also Coulomb between electrons i and j and the fifth is repulsion between nucleus A and nucleus B.[73]"

It then reduces to the following equation due to some estimations we make about molecular systems. And the Born-Oppenheimer Approximation is then made.

$$\hat{H}_{elec} = -\sum_{i=1}^{N} \frac{1}{2}\nabla_i^2 - \sum_{i=1}^{N}\sum_{A=1}^{M} \frac{Z_A}{r_{iA}} + \sum_{i=1}^{N}\sum_{j>i}^{N} \frac{1}{r_{ij}} \tag{23}$$

In the Born-Oppenheimer approximation, Ψ is considered explicitly dependent only on r_i, while parametrically dependent on R_i. This requires solving the Schrödinger Equation first at a fixed R_i [15] while we consider all nuclei frozen and classical due

to the nuclei being much heavier and thus slower than the orbiting electrons.

$$\hat{H}\Psi(r_i; R_I) = E(R_I)\Psi(r_i; R_I) \tag{24}$$

1.2.1 Wave Function and the Nucleus of an Atom

"Schrödinger originally interpreted his Ψ function in the following way. The electron is not a localized charge within the atom, but charge and mass are "smeared" over a certain region. The density of charge is assumed to be proportional to $\Psi\Psi*$, the "norm", or square of the amplitude of the Ψ function.[31]" Here, Ψ_i, describes the orbitals of a sordid quantum mechanical system using mathematics. The following wave function is called a Slater Determinant and is made up of orbitals as the rows and electrons as the columns. The Slater determinant is made entirely of orbitals. Electrons are there only as their coordinates and are simply arguments of the orbitals. The Slater determinant is used because of independent particle motion and the fermion antisymmetry. The vector $\vec{r}$, is the coordinate for that electron and the normalization factor, N, is the number of electrons in the system. For transition metals and diradicals, it is extremely advantageous to have a combination of determinants in order to calculate a good approximation. This is in consistentency with the sixth postulate of Quantum Mechanics.

$$\begin{aligned} \Psi(\vec{r}_1, \vec{r}_2, \cdots, \vec{r}_N) &= \frac{1}{\sqrt{N!}} \begin{vmatrix} \psi_1(\vec{r}_1) & \psi_1(\vec{r}_2) & \cdots & \psi_1(\vec{r}_N) \\ \psi_2(\vec{r}_1) & \psi_2(\vec{r}_2) & \cdots & \psi_2(\vec{r}_N) \\ \vdots & \vdots & \ddots & \vdots \\ \psi_N(\vec{r}_1) & \psi_N(\vec{r}_2) & \cdots & \psi_N(\vec{r}_N) \end{vmatrix} \qquad (25) \\ &= \frac{1}{\sqrt{N!}} \det |\psi_1(\vec{r}_1)\psi_2(\vec{r}_2)\cdots\psi_N(\vec{r}_N)| \qquad (26) \end{aligned}$$

The nucleus can be studied solely by classical electromagnetics via the Born-Oppenheimer approximation.

1.2.2 Molecular Orbitals

Molecular orbitals are linear combinations of atomic orbitals that give us an idea of how an electron in a molecule behaves. It is derived from the quantum mechanical wavefunction by way of the linear combination of atomic orbitals (LCAO) method. A general form of a molecular orbital can be written in the following way, where χ_i are the individual atomic orbitals and c_{ij} are the coefficients. The coefficients can be calculated numerically via the variational principle.

$$|\phi_j\rangle = \sum_{i=1}^{n} c_{ij} |\chi_i\rangle \tag{27}$$

By multiplying these molecular orbitals, we form what is called a configuration. A configuration is a product of molecular orbitals whose equation is displayed below.

$$|\Phi_i(1...N)\rangle = [|\phi_{i1}(1)\rangle \wedge |\phi_{i2}(2)\rangle \wedge ... |\phi_{iN}(N)\rangle] \tag{28}$$

When these configurations are added together, a state is formed. A state is a function which sums the configurations and contains all accessible physical information about the system, as mentioned previously in the postulates of Quantum Mechanics[45].

$$|\Psi_\alpha(1...N)\rangle = \sum_i c_i^\alpha |\Phi_i(1...N)\rangle \tag{29}$$

Where α is the number of spin orbitals.

Although speculated eariler by Mulliken and Coulson, yet proposed by S. F. Boys

in 1950, a basis set is a set of one-particle functions used to describe the wave function using molecular orbitals[9]. These molecular orbitals are a linear combination of atomic orbitals. There are two types of orbitals most widely used: Slater-Type Orbitals (STOs) and Gaussian-Type Orbitals(GTOs). The most common being STOs. The difference between the two is the following.

1.2.3 STO

The STOs are more accurate but less efficient computationally. They have the general form

$$\psi_{\alpha,n,l,m}(r,\theta,\phi) \quad = \quad N_{\alpha,n}Y_{l,m}(\theta,\phi)r^{n-1}e^{-\alpha r} \tag{30}$$

1.2.4 GTO

These orbitals are generally near the nucleus and do not have a cusp. The distance from the nuclei decay is on the order of e^{-ar^2} and these formulas tend to be much more simpler than their STO counterparts. The formula describing GTOs is written as

$$\psi_{\alpha,n,l,m}(r,\theta,\phi) \quad = \quad NY_{l,m}(\theta,\phi)r^{2n-2-1}e^{-\alpha r^2} \tag{31}$$

1.3 Basis Sets

1.3.1 3-21G

In the split-valence basis set, a double-zeta (α) only calculated for the valence orbital in the system. The inner-shells are not ignored but they are linear combinations of GTOs, making it a relatively small basis set.

1.3.2 6-31G

A bigger basis set, John Pople's split-valence double-zeta (α) above, named 6-31G is defined for atoms H through Zn on the periodic table of elements. The 6-31G*(6-31G(d)) is 6-31G with d polarization functions on all atoms except hydrogen and 6-31G**(6-31G(d,p)) is 6-31G* with p polarization for hydrogen. In general, the larger the basis set, the more accurate. Critics such as Angela Wilson contend that DFT is less dependent on basis set size than wavefunction methods.

1.3.3 Hund's Rules

The highest multiplicity has the lowest energy. Each electron will occupy an orbital by itself until all orbitals in that subshell is filled. These electrons will all have the same spin. After filled with single electrons, then another electron with opposite spin can share the orbital with the original electron. The largest value of spin multiplicity, L=2×S+1 or $L = 2S + 1$ will yield the lowest energy, where S is spin $\pm\frac{1}{2}$. The negative sign is spin down and the positive sign is spin up. This is always the case with the exception being j-j coupling in heavier elements.

1.3.4 Energy Calculations

In Quantum Mechanics, we learn that it is a lot easier to measure the energy of a particle than to observe its location. When we discuss energy at the quantum chemical

level, we should realize that this is the potential and kinetic energy possessed by the electrons in the atoms[22]. Electrons in different orbitals can have different ways of interacting. This can depend on the spin, placement, and orbital type. For a system of two electrons in different orbitals, they can be paired by states called singlet and triplet. The energy that these two electrons conjure is called the Singlet-Triplet Split $= E_{triplet} - E_{singlet}$.

1.4 Density Functional Theory

Contrary to wavefunction theory, Density Funtional Theory (DFT) starts with a focus on the electron density ρ, as opposed to the the wave function, Ψ. The energy of the molecule is calculated by a functional, which in simplest terms mean a function of another function that produces a numerical result. Scientists Hohenberg and Kohn proved that the ground-state energy of a manybody system in an external potential is a functional of the electron density. This energy is

$$E[\rho] = \int \rho(r) v_{ext}(r) d^3r + F[\rho] \tag{32}$$

and $v_{ext}(r)$ is the static potential caused by the Coulomb interaction of the nucleus and electrons. The functional, F[ρ] is a universal functional of electron density $\rho(r)$. While a function maps a set of numbers to another set of numbers, a functional map's a function to a number via integration in our case[13].

$$F[\rho] = \frac{1}{2} \int \int \frac{\rho(r)\rho(r)'}{|r - r'|} d^3r d^3r' + T_s[\rho] + E_{xc}[\rho] \tag{33}$$

The kinetic energy for the system is

$$T_s[\rho] = \langle \phi_i | - \frac{1}{2} \sum_i^N \nabla_i^2 \, | \phi_i \rangle \tag{34}$$

The kinetic energy term can also be written as $T_0[\rho]$.

$$T_0[\rho] = -\frac{1}{2} \sum_i \int \Psi_i^*(r) \nabla^2 \Psi_i(r) d^3 r \tag{35}$$

The electron density can be expressed as

$$\rho(r) = \sum_i^N |\phi_i(r)|^2 \tag{36}$$

By taking the functional derivative of E[ρ] with respect to ρ(r) and setting it equal to zero, the following one particle Kohn-Sham equation is produced

$$\left(-\frac{1}{2} \nabla^2 + V_{eff}(\vec{r}_1) \right) \phi_i = \epsilon_i \phi_i (i = 1, 2, ...N) \tag{37}$$

The effective potential v_{eff}(r) can then be approximated, yielding

$$v_{eff}(\vec{r}) = v_{ext}(\vec{r}) + \int \frac{\rho(\vec{r}')}{|\vec{r} - \vec{r}'|} d^3 \vec{r}' + v_{XC}(\vec{r}) \tag{38}$$

where v_{XC} is the functional derivative of the exchange-correlation energy correction term.

$$v_{XC} = \frac{\delta E_{XC}}{\delta \rho} \tag{39}$$

One of the principle challenges of density functional theory is the determination of the term v_{XC}, which "defines a local potential that takes exact account of both exchange

and correlation[79]." An approximation to the exchange-correlation energy, The Local Density Approximation (LDA) is defined as

$$E_{XC}[\rho] = \int f[\rho(\mathbf{r})]\mathbf{d^3r}, \tag{40}$$

noting especially $f[\rho(r)]$, which is the exchange-correlation functional of the uniform electron gas. In the uniform gas case (UEG), the UEG exchange can be described the following way:

$$f[\rho(r)] = -\frac{9}{8}\alpha\left(\frac{3}{\pi}\right)^{1/3}\rho(r)^{4/3} \tag{41}$$

The electronic energy is determined by the total electron density. Because the density is a bi-linear form of orbitals, not just the sum of orbials (but can be expressed as the sum of squared orbitals), DFT only needs to compute each MO (molecular orbital), resulting in a computational complexity of N. The Computational Complexity of the wave function is $N! = N^N$, because the wave function contains all of the electron positions. Once the Kohn-Sham molecular orbitals are solved for, then the kinetic energy, T_s is exactly obtained from them, and also the electron density. Once the electron density is obtained we plug it in f[ρ] and obtain the energy. Simple approximations are made for this term. The integral of f above is called the Local Density Approximation (LDA).

1.5 Bonds

A covalent chemical bond is formally defined as a quantum effect of sharing valence electrons between two atoms so that it leads to a lowering of the energy of the bonded

atoms compared to the energy if they were unbonded. There are two main types of covalent bonds, π and σ. The sigma bond is formed by overlap of two s orbitals or one s and one p. Two p-orbitals overlap and form a π bond. The σ bond is stronger than a π bond and is also responsible for the shape of the molecule. It can be formed by head on overlapping of atomic orbitals. The π bond brings atoms closer to each other in distance. If the spins in a pair of electrons are different (anti-parallel) then the bond will form. If the spins are the same (parallel), then the bond will not form in general, but a π bond can form with leftover p-orbitals of both atoms.

Mayer's bond order follows from the expansion of the second order density matrix G(1,2), the first order of which is the product n(1)n(2) - $\gamma(1;2)\gamma(2;1)$. The quantum exchange effects that are responsible for bonding come from the second term above. Expanding this second term in MOLCAO (Molecular Orbital Linear Combination of atomic orbitals), integrating over spacial variables and grouping the terms with two different atoms gives the Mayer bond order[44].

1.5.1 Spin of an Electron

Electron spin was discovered by Pauli and is generally in the field written as $\alpha(1)$, spin up and $\beta(1)$, spin down. Particles, such as electrons have a spin of $\frac{1}{2}$. Electrons are fermions while particles having spin 1 are bosons.

2 THE LITERATURE REVIEW

Quantum chemistry calculation methods are useful for describing PAH characteristics. Density Functional Theory (DFT) offers the most computational efficiency with respect to performance and accuracy. Popular belief insists that due to the somewhat open-shell nature of these PAHs, an unrestricted approach is needed when using DFT to study these systems[16]. Lischka et al address the problem of spin contamination

using an expression found in their work[16].

The reason the KP16/B13 functional is so advantageous is due to its handling of the left-right correlation, which is responsible for partly decoupling the bond electron pairs, making them unpaired, or odd[35]. These electrons stay localized in the atomic areas of the system due to this effect. When this effect is amplified, it gives rise to the formation of polyradical states within the system, which condensed matter scientists call narrow-band electron localization. Unfortunately, these physical properties cannot be characterized at the single-determinant self-consistent field level. It is from this view that one can observe that the formation of atomic population of localized electrons, or APELE in singlet systems is a solely correlation-based phenomenon.

On page 1629 of the paper titled, Polyradical Character of Triangular Non-Kekule Structures, p-Quinodimethane-Linked Bisphenalenyl, and the Clar Goblet in Comparison: An Extended Multireference Study, by Lischka et al., Figure 3 shows the effectively unpaired electrons on each atom. They use the high-level ab initio wavefunction method, π-MR-CISD. We perform calculations with our functional KP16/B13 and odd electron population method called atomic population of localized electrons (APELE). The advantage of APELE is computational efficiency[16].

2.1 Configuration Interaction

The post-Hartree-Fock method which includes instantaneous electron correlation, Configuration Interaction (CI), solves the nonrelativistic Schrodinger equation. Also called configuration mixing (CM), CI uses a linear variational wave function composed of N-electron trial functions. Coefficients in the linear equation are optimized and if the N-electron wavefunctions are complete, an exact calculation of the energy can be obtained - full CI is then achieved[21].

2.2 Multiconfiguration Self-Consistent Field

A general form of the MCSCF wavefunction is given.

$$\Psi_{MCSCF} = \sum_{K} A_K \Phi_K \tag{42}$$

$$\Phi_K = A\left\{\prod_{i \subset K} \phi_i\right\} \tag{43}$$

$$\phi_i = \sum_{\mu} \chi_\mu C_{\mu i} \tag{44}$$

Basic, barebones CI uses the SCF wavefunction as a reference function for getting the configuration state functions while MRCI starts with a linear combination state-functions MCSCF wavefuction Φ_K, used to create more configuration state functions. Configuration state functions differ in the way the electrons are distributed among the molecular orbitals.

MR-AQCC[40] is one of the most popular methods because of how simple they are. It is very similar to MRCI[41] and available in the following programs: COLUMBUS[39], MOLPRO[74], and MOLCAS[33].

2.3 Natural Orbitals

Natural Bond Orbitals (NBOs) have the highest possible percentage of the electron density, ideally close to 2.0000, giving the most accurate possible "natural Lewis structure" of Ψ. A high percentage of electron density, denoted by ρ_L, often found to be in greater than ninety-nine percent of common organic molecules, correlate with an accurate natural Lewis structure. Basically, natural orbitals[75], are defined as the eigenfunctions of the correlated density matrix. This is very convenient when calculating unpaired electron density[51].

A mathematical description of the natural orbitals Θ, of a wavefunction Ψ can be expressed as the eigenorbitals of the first-order reduced density operator Γ,

$$\Gamma\Theta_k = p_k\Theta, where(k = 1, 2, ...) \tag{45}$$

In the above equation, p_k is the population or occupancy of the eigenfunction Θ_k for the molecular electron density operator Γ of Ψ. The density operator is just the 1-electron "projection" of the full N-electron probability distribution, $|\Psi|^2$ which helps elucidate characteristics of the 1-electron subsystems of, Ψ the total wavefunction. It is the same small γ used to define bond order and density of odd electrons, however; here γ must be calculated via the correlation method to get the NO. In Kohn-Sham theory, the single determinant expression of γ has no explicit correlation in it and the Kohn-Sham orbitals are not the natural orbitals.

Natural Orbitals are the closest to the Lewis structures as you can get for a chemical system, but note that Lewis structures are very approximate. Scientists use of this way of describing the system is incomplete. This is why we use Slater Type Orbitals (STO) or Gaussian Type Orbitals (GTO) because they have a proven track record of success over many years[23]. NOs are usually not used for the actual SCF calculation but formed and used after the SCF calculation is completed for the sake of having a chemical description and interpretation.

2.4 Properties of Polycyclic Aromatic Hydrocarbons (PAH)

Hydrocarbons are stable at room temperature because the C-H bond is strong. The carbon atom likes to form long single bonds that form chains and/or rings with hydrogen attached. No other element on the periodic table does this[24].

Investigating potential properties of certain specific PAHs is very important. Knowing whether or not a PAH can be stabilized is worthy of investigation. The

study of these graphene-like PAHs are in the realm between molecular and macromolecular structures.

Some examples of PAHs include carcinogens (burnt food when we BBQ or smoke) and moth balls. Applications of these are materials science studies to achieve semiconductors and sensors. They also have a large radius of gyration. In classical physics, spheres with larger radius of gyration tend to resist rotation longer than spheres with a smaller radius of gyration. One of the important questions is which computational theory is the best for calculating these? Radicals are very significant in combustion reactions, atmospheric chemistry, and polymerization and plasma chemistry, biochemistry, and many other chemical processes. A good amount of natural goods are made by radical-generating enzymes. In living organisms, the radicals superoxide and nitric oxide and their reaction products regulate many processes: control of vascular tone and blood pressure.

Diradicals have higher reactivities and shorter lifetimes. In a broader definition diradicals are even-electron molecules that have one fewer bond than the number permitted by the standard rules of valence. Fundamentally, magnetism, optics, and conductivity can be considered interrelated properties resulting from unpaired electrons[18].

One major issue with PAHs is the limitation in their volume. It is quite difficult to grow them from molecular to the major macromolecular range because an increase in molecular weight, in general, decreases the solubility of the molecule. This has a tendancy to also increase side reactions. However, in 2008, Mullen et al were able to sythesize nanoribbon-like PAHs 12 nm in length. These newly created PAHs' properties have not been studied and could be similar to graphene. Expanding PAH volume could have a great impact on producing conjugated macromolecules[4].

From the previous chapter recall the section on bonding - sigma bonds can form

by overlapping orbitals. Methane is a popular example. Also, π stacking (called $\pi - \pi$ stacking) refers to attractive, noncovalent (not sharing an orbital) interactions between aromatic rings, since they contain π bonds. There are several types: sandwich, t-shaped, and parallel-displaced. To quote Akasaka et al, "Despite intense experimental and theoretical interest, there is no unified description of the factors that contribute to π stacking interactions[2]." This can be somewhat challenging to describe geometrically. This is very hard to describe computationally, therefore this is also a problem that we could look into. Could odd electron calculations provide more insight?[16]

2.5 Atomization Energy

Atomization energy can be defined as the energy needed to decompose a molecule completely into a gas state of isolated atoms. In most regular reactions, heat will help break several bonds. When dealing with combustion reactions, heat breaks most of the bonds. Of course, when there is an abundance of heat, that is the ideal environment for all the bonds to be broken to free all of the atoms and have them remain isolated. As the energy becomes greater than the bond energy of all bonds, this is atomization. Usually, such energy differences can be estimated using imaginary thermodynamical cycles of Hess and thermodynamic tables for enthalpies of formation.

Atomization energy is the energy involved with the forming of 1 mole of atoms in the gas state from 1 mole of gas element to its standard state of matter under basic conditions. The atomization energy (AE), given system AB_2C, is

$$AB_2C = E(AB_2C) - E_a - 2E_b - Ec$$

2.6 Atomic Population of Effectively Localized Electrons - APELE

Studying PAHs can uncover more knowledge regarding the Exchange Correlation. This pursuit of knowledge leads us to look at the properties of the electron density. For analysis of radical character, Lischka et al, use (a) NO (natural orbital) occupations as computed from the MR-AQCC (multireference averaged quadratic coupled cluster) density and (b) the unpaired density and the number of effectively unpaired electrons (NU) as originally introduced by Takatsuka et al. as the distribution of "odd" electrons. This method was further developed by Staroverov and Davidson. In order to emphasize the contributions from orbitals with occupation near one and suppressing contributions that are nearly doubly occupied or nearly occupied, the nonlinear formula of Head-Gordon is used in which n_i is the occupation of the ith NO and M is the total number of NOs[16].

$$N_U = \sum_{i=1}^{M} n_i^2 (2 - n_i)^2 \tag{46}$$

To get the unpaired electron density, one would simply multiply the right side of the equation by the NO orbital density i, which is the square of the NO orbital i.

Disregarding electron correlation, ground state singlet orbitals of the systems can be doubly occupied by an electron pair of spin up/down. This picture has helped in the comprehension of how stable molecules are constructed electronically via restricted Hartree-Fock (RHF) theory. When the concept of electron correlation is introduced, the model breaks down. The orbital is divided into two orbitals which the pair of electrons occupy separately. "An electron pair will thus be split spatially to assume a partial odd-electron character even in a singlet ground-state molecule. The nature of such split electron pairs should have a particularly significant bearing

on the properties of the so-called singlet diradical species as well as the transition state of certain concerted reactions[68]."

The density of atomic population of localized electrons (APELE[57]) is

$$D_\sigma(\mathbf{r}) = \rho_\sigma(\mathbf{r})[\mathbf{1} - \mathbf{N^{eff}_{X\sigma}}(\mathbf{r})] \tag{47}$$

$N^{eff}_{X\sigma}(\mathbf{r})$ is called effective partial normalization of the exchange hole within a region of roughly atomic size in a molecule. The smaller that $N^{eff}_{X\sigma}(\mathbf{r})$ is, the stronger the non-dynamic correlation is at $\mathbf{r}$, and the larger the APELE density $D_\sigma(\mathbf{r})$. The spin-summed odd-electron (APELE) density is

$$D_u(\mathbf{r}) = \mathbf{4a^{op}_{nd}} \sum_\sigma \rho_\sigma(\mathbf{r})[\mathbf{1} - \mathbf{N^{eff}_{X\sigma}}(\mathbf{r})] \tag{48}$$

The SCF-optimized linear coefficient multiplied by the opposite-spin Becke05 non-dynamic term a^{op}_{nd} is 0.526. The atomic population, $F_r(A)$, of APELE is

$$F_r(A) = \int_{\Omega_A} D_u(\mathbf{r})\mathbf{dr}. \tag{49}$$

The Ω_A term is the subregion of atom "A" in the chemical system. Using Becke's grid integration scheme allows us to define atomic regions simply, with grid space atomic subgroups[57]. The numerical grid is an atom-centered un-pruned ultra-fine grid with 128 radial and 302 angular points per shell within Becke's relative weights integration scheme[8].

The main principle on analyzing odd electrons (OE) is that the bigger the population of OE on the atoms, the more unpaired electrons have in the molecule which indicates large effects of nondynamic correlation (i.e. multireference character) in said molecule.

Even though the structure of the multireference wave functions are complicated,

reconciling the polyradical nature is trivial when it comes to using unpaired electron density calculations or APELE[16].

2.7 Delocalization

Delocalization is defined as molecular orbital of electrons that extend over several adjacent atoms. Standard ab initio quantum chemistry methods lead to delocalized orbitals, that generally extend over the whole molecule and are symmetrical with the molecule. Localized orbitals are usually described as linear combinations of delocalized orbitals, given by a unitary transformation.

A short and basic definition of Kekule structure is a Lewis structure without the lone pairs. In the context of a simple aromatic ring of benzene, delocalization of six π electrons over the C_6 ring is often indicated by the drawing of a circle. Six C-C bonds are equal distances apart and is one indication that π electrons are delocalized - if the structure has isolated double bonds alternating with discrete single bonds, the bond probably has alternating longer/shorter lengths. In VB (valence bond) theory, delocalization in benzene is represented by the resonance structure.

Another description of delocalization also exists in solid metals. Metallic structure consists of aligned positive ions (cations) in an ocean of delocalized electrons. Electrons are able to move through the structure and we start to see the electronic properties such as conductivity. In this case, delocalized suggests that the electrons do not belong to any one metal nucleus but can spread all through the metal. And you can see that when we talk about delocalization, we also mean a little bit of this as well.

In diamond, it is the opposite. The story is that the four outer electrons of each carbon are 'localized' between the atoms in covalent bonding. The electrons in diamond do not move, therefore it does not conduct electricity. Observations indicate

that graphite's carbon atoms' electrons only occupy three of its outer energy levels, thus forming covalent bonds with three other carbon atoms in a plane and giving one freely moving electron to a group of delocalized electrons for the purpose of chemical bonding. These electrons travel about the plane. Graphite follows this model of producing electricity.

2.8 Mayer's Bond Order

Bond order, bond index, and electron valence are essential to comprehending chemistry. These ideas are involved in all diagramed chemical structures and core to chemistry education. Combined with quantum theory and electronic strucuture, they prove to be very useful and are nonetheless very important[10].

There are several scientists that have created a formulation of bond order: Coulson, Mulliken, Wiberg. Chemists' basic definition of bond order is $B = \frac{N_{bond} - N_{antibond}}{2}$. Bond order was first defined as the off-diagonal matrix element of the Coulson charge bond order matrix. One could then pick out the π-component of the bond order between two atoms of a conjugated system. Bond order is useful in describing how much π-bonding between the centers of the two systems that are bonded. One could also call it the π-electron bond order since its highest value is 1 for the ehtylene system, while recalculating larger numbers for more delocalized π-electron atoms[44].

The simplest molecular orbital calculation of bond order comes from Coulson regarding pi-orbitals at the Huckel level. The Mayer definition of bond order is simply an extension of the Wiberg index. It also works on inorganic systems such as sulfur-nitrogen rings, halogen-oxide molecules, and transition metal dichloride molecules[10].

$$B_{AB} = \sum_{s}^{onA} \sum_{t}^{onB} (\mathbf{PS})_{st} (\mathbf{PS})_{ts} \tag{50}$$

In the above equation, $\mathbf{S}$ is the atomic orbital overlap matrix and the $\mathbf{P}$ matrix is

the molecular orbital LCAO (linear combination of atomic orbitals) coefficient matrix.

Mayer bond order can be interpreted as the Wiberg index expanded. Homonuclear diatomics result in integer values for small basis sets and non-integers for large basis sets and complex molecules. Information about how ionic the bond is, delocalization and multicontour effects is also given in calculations[10].

2.9 Possible Research Paths

According to the literature, there are several research inquiries of interest that our calculations can elucidate.

It could be possible that the implementation of the SCAN functional into the xTron software may help to improve the KP16/B13 functional. The SCAN functional is a recently invented by Perdew et al claims to be the only functional capable of predicting "band gap (or absence thereof) and the spin moments of the undoped and doped cuprate high-temperature superconductor materials, without free parameters."[59] Studying it may bring up new ideas to improve KP16/B13. This research investigation is fully described in the chapter titled ***Methodology of Study 1***.

Discovering how well KP16/B13 performs with respect to other functionals on hydrocarbon chemistry as well as a specific set of organic molecules would be a good way to see if there is merit in advancing a study of PAHs with the APELE method. A benchmarking study of KP16 is explained in the chapter titled ***Methodology of Study 2***.

It may also be possible that our APELE method can successfully capture the bi- or polyradical character of PAHs. APELE can possibly show connections in other organic chemical systems and shed more light on the aromaticity of organic molecules. Studying fractional charges in chemical systems using DFT should assist in the comprehension of properties of the fuctional as well[14].

Interest has also been garnered in determining which form is dominating in the ground state. A study of which isomer contains a larger biradical character would also be of benefit.

According to Clar's aromatic sextet rule, for benzenoid PAHs, the molecule with more aromatic sextet rings has more aromatic stabilization energy. The more rings, the more stable it will be. There should be energy going from greatest to least[16]: phenalenyl, triangulene, and π-extended triangulene; heptazethrene, 1,2:9,10 - dibenzoheptazethrene, and 5,6:13,14-dibenzoheptazethrene; p-quinodimethane - linked bisphenalenyl and clar goblet all separately.

Our colleagues in the field are also curious about if triangular structures phenalenyl, triangulene, and π-extended triangulene[16] have a nondegenerate spin state that increases with increasing molecular size as predicted by Ovchinnikov's rule. One would want to know if this is in agreement with ESR measurements of tri-tert-butyle-substituted phenalenyl, triangulene, and triangulene derivative.

Also of note would be if KP16/B13 DFT LC (local correlation) treatment reproduces subtle changes in singlet-triplet splittings for heptazethrenes. But preliminary results show the opposite trend that Lischka et al see when plotting our singlet-triplet energy calculations of the systems. This investigation is discussed in the chapter titled ***Methodology of Study 3***.

The simplest system which illustrates the strong correlation effect is the 1-D linear H-atom chain. It changes from a metal to a Mott insulator when the iteratomic distance is increased evenly from equilibrium. It would be of interest to observe what a 1-D linear carbon atom chain would manifest: such as any strong correlation effects or enhanced static correlation interaction. One important piece of information that would be extremely beneficial is if carbon atoms could serve as a basic prototype for

static correlation in organic molecules. This study is revealed in the chapter titled ***Methodology of Study 4***.

2.10 Limitations and Assumptions of the Research

2.10.1 Computational Limitations

With supercomputing power in limited supply worldwide, it is important to recognize what is possible with respect to calculations. Fortunately, the efficiency can be partially quantified by the Scaling Law: $R = A * N^B$. In fact, this is the law that most computational chemistry methods use to ascertain performance. Computational resources R which are time and memory, increase proportionally by A multiplied by the system size N to the power of B. The variable A can be lowered by a number of different approximations. More importantly, the size of the system N is what is paid the most attention to. In DFT, N is often the number of molecular orbitals[3].

2.10.2 Algorithmic Limitations

Now that DFT is a lot more popular and developed than previous years, comprehension of errors becomes ever so critical. Most of the errors in DFT are due to DFTs approximation of the exchange-correlation functional. Further understanding these errors and how they address the physics can drastically improve DFT in the long run[14].

As we see in Figure 1, experimentalists must continue to be a resource for scientists developing DFT for comparing results in order to reduce these errors. In the 1990s, John Pople and coworkers used experimental data and were able to get results to chemical accuracy (1 kcal/mol)[14].

DFT is less accurate than configuration interaction and some other methods. Some of the sources of errors arise from the following:

1) Exchange and potential energy formulations that are inappropriate.

2) How the functionals are built.

3) Choosing the wrong basis set or pseudo-potential.

4) Wrong polarization assumptions in density and molecular orbitals.

5) The handling of dispersion.

In odd electron stretched systems like He_2^+ and $(H_2O)_2^+$, significant errors arise when the distance of electrons from the nucleus increases. More attention is now being paid to the functionals as a consequence of the discovery that this is due to the functionals themselves[14].

Metallic solids may be prone to delocalized density errors as well as with closed-shell organic molecules. Some isomers of the *-enes (specifically [10]annulene[34]) with twisted conformations, may have delocalized density. With respect to the CCSD(T) calculations, GGA DFT functionals give a higher density value of the twisted confirmation. The error is large and is caused by GGA functionals not giving a high enough energy for delocalized charge distributions. Density functional performance is shown to be correlated with odd electron systems such as CH_4^+. Many authors agree that

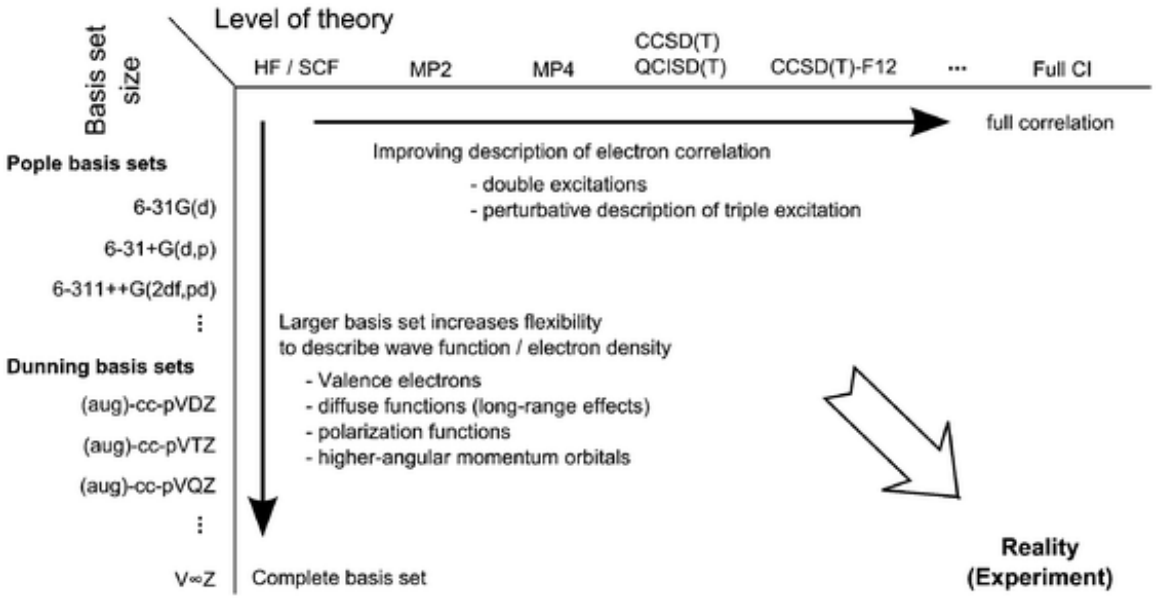

Figure 1: As you go horizontally from HF/SCF theory to Full CI theory, improvement of the description of electron correlation increases along with double excitations and the pertubative description of triple excitations. Going vertically downward on the graph shows that larger basis sets increase the ability to describe the wave function and electron density[71].

the comprehension of delocalization error thus far is an issue based on fundamental chemistry knowledge as evidenced by the mathematics[14]. These notions have clear-cut physical effects. One should also reconcile with the idea that the various different locations of the electron density can be caused by inadequacies in the functional and not the fundamental physics[14].

Under these conditions, preservation of dispersibility and a planar morphology for large PAHs has been very challenging. PAHs and organic molecules in general take long to calculate in part because of their size. PAHs are also good because it's possible to modify their solubility.

3 METHODOLOGY OF STUDY 1

The SCAN functional is the first meta-generalized-gradient (meta-GGA) approximation which is fully constrained, adhering to all seventeen constraints that a meta-GGA can have; while also exact or close to for "appropriate norms" such as rare-gas atoms and nonbonded interactions. By implementing this functional, we are hoping to learn from it and also compare our future development with it. In this study, the exchange-correlation energy was calculated for an implemented strongly constrained and appropriately normed (SCAN) semilocal density functional for several chemical systems[64].

3.1 SCAN DFT: An Introduction

The SCAN functional is a computationally efficient and is good at solving covalent, metallic, ionic, hydrogen, as well as intermediate-range van der Waals bonding. In this functional, the exchange correlation energy in SCAN is a combination of LDA (Local Density Approximation), GGA (Generalized Gradiant Approximation), and meta-GGA (meta-Generalized Gradient Approximation).

3.2 The Scientific Problem: SCAN Functional via HPC

In this study, the exchange-correlation energy E_{xc}, for a strongly constrained and appropriately normed (SCAN) semilocal density functional [63] for several chemical systems was calculated. In general, the exchange correlation energy is the additive sum of the exchange energy and the correlation energy,

$$E_{xc} = E_x + E_c \tag{51}$$

Since we have a specific case of a high-density spin-unpolarized limit of the exchange correlation factor $E_c = 0$, we only have to calculate E_x.

$$E_x[n] = \int d^3r n\epsilon_x^{unif}(n)F_x(s,\alpha) \tag{52}$$

This is done by first calculating the exchange-correlation enhancement factor F_{xc}, for a strongly constrained and appropriately normed (SCAN) semilocal density functional [63] . In comparison to the exchange correlation energy, the exchange correlation enhancement factor F_{xc}, is the additive sum of two components: the exchange enhancement factor, F_x and the correlation enhancement factor, F_c resulting in the equation

$$F_{xc} = F_x + F_c \tag{53}$$

Again, because of this specific case of a high-density spin-unpolarized limit of the exchange correlation factor, $F_c = 0$, making $F_{xc} = F_x$. The exchange enhancement factor is given by

$$F_x(s,\alpha) = \{h_x^1(s,\alpha) + f_x(\alpha)[h_x^0 - h_x^1(s,\alpha)]\}g_x(s) \tag{54}$$

3.3 Solution

Mathematically construct the exchange enhancement factor F_x using interpolation/extrapolation function

$$f_x = \exp\left\{\left(\frac{-c_{1x}\alpha}{1-\alpha}\right)\theta(1-\alpha)\right\} - d_x\exp\left\{\left(\frac{c_{2x}\alpha}{1-\alpha}\right)\theta(\alpha-1)\right\} \tag{55}$$

and $\theta(x)$, which is a step function we interpolate between $\alpha = 0$ (for covalent single bonds) and $\alpha \approx 1$ (for metallic bonds),

$$g_x(s) = 1 - e^{-a_1 s^{-1/2}} \tag{56}$$

The variable s is the dimensionless density gradient:

$$s = \frac{|\nabla n|}{[2(3\pi^2)^{1/3} n^{4/3}]}, \tag{57}$$

$h_x^0 = 1 + k_1$, and c_{1x}, c_{2x}, d_x, k_1, h_x^1, and a_1 are adjustable parameters while θ is a basic heaviside step function[65]. Now, $\theta(1-\alpha)$ and $\theta(\alpha - 1)$ can be 0 if negative, $\frac{1}{2}$ if 0, or 1 if positive. A graph of F_x versus s from the literature is shown in Figure 2. Confirmation of the same plot was done in MATLAB and shown in Figure 3.

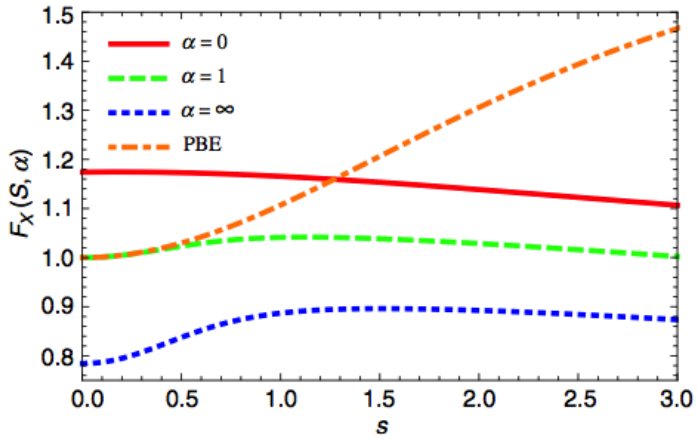

[64]

Figure 2: The SCAN exchange enhancement factor, F_x with respect to s[64].

Therefore, making

$$F_{xc} = F_x(s,\alpha) = \{h_x^1(s,\alpha) + \left[\exp\left\{\left(\tfrac{-c_{1x}\alpha}{1-\alpha}\right)\right\}\theta(1-\alpha) - d_x \exp\left\{\left(\tfrac{c_{2x}\alpha}{1-\alpha}\right)\right\}\theta(\alpha-1)\right][h_x^0 - h_x^1(s,\alpha)]\}g_x(s) \tag{58}$$

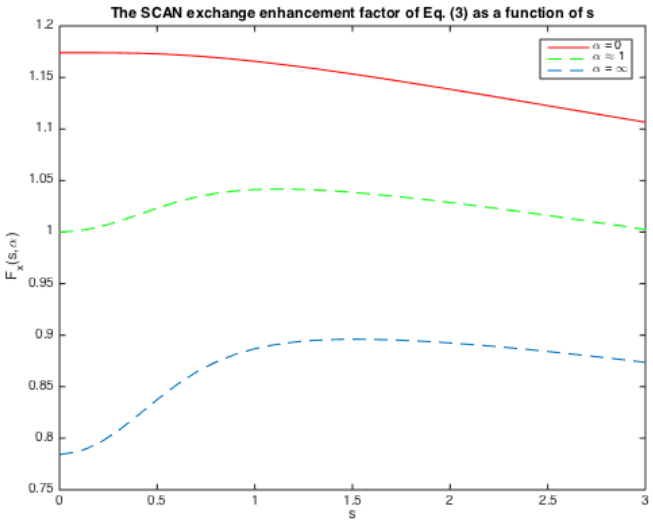

Figure 3: The reproduced exchange enhancement factor, F_x with respect to s, using MATLAB.

The spin unpolarized variable

$$\alpha = \frac{\tau - \tau^W}{\tau^{unif}} \tag{59}$$

where

$$\tau = \frac{1}{2}\Sigma_i^{occ}|\psi|_{i,\sigma}^2, \tag{60}$$

which is calculated internally in the xTron code,

$$\tau^W = \frac{|\nabla n|}{8n} \tag{61}$$

is the exact kinetic energy for any one-electron system called the Weizsaecker kinetic energy density [13], and

$$\tau^{unif} = \frac{3}{10}(3\pi^2)^{2/3}n^{5/3}, \tag{62}$$

is the kinetic energy density. So,

$$\alpha = \frac{\tau - \frac{|\nabla n|}{8n}}{\frac{3}{10}(3\pi^2)^{2/3}n^{5/3}}. \tag{63}$$

Now, with certain terms substituted, our equation for the exchange correlation factor now looks like the following.

$$F_{xc} = \left\{ h_x^1(s,\alpha) + \left[\exp\left\{ \left(\frac{\tau - \frac{|\nabla n|}{8n}}{-c_{1x}\frac{3}{10}(3\pi^2)^{2/3}n^{5/3}} \right) \right\} \theta(1-\alpha) - d_x \exp\left\{ \left(\frac{\tau - \frac{|\nabla n|}{8n}}{c_{2x}\frac{3}{10}(3\pi^2)^{2/3}n^{5/3}} \right) \right\} \theta(\alpha - 1) \right] [h_x^0 - h_x^1(s,\alpha)] \right\} g_x(s) \tag{64}$$

Next, a numerical integration is performed to calculate the product of the ground-state electron density $n(\vec{r})$, the exchange energy per particle of a uniform electron gas $\epsilon_x^{unif}(n)$, and the exchange enhancement factor $F_x(s,\alpha)$.

The spin-polarized values of τ, n, and ∇n are calculated internally and passed in from the inner workings of the xTron program. Only one spin-polarized value is needed (τ): two times its spin up or spin down value. The exchange energy per particle of a uniform electron gas is calculated by

$$\epsilon_x^{unif}(n) = -\left(\frac{3}{4\pi}\right)(3\pi^2 n)^{1/3}, \tag{65}$$

where n is the electron density that depends on position. And as previously stated, when n is integrated it should equal the total number of electrons in the system.

The following is a code snippet of the Fortran subroutine of the SCAN functional implemented into xTron. The code is displayed in its entirety in the Appendix of this dissertation.

```
! loop over the number of grid points
do i = 1,NG
    RA   = RhoA(i)
    RB   = RhoB(i)

    GAA = DRA(i,1)*DRA(i,1) + DRA(i,2)*DRA(i,2)
    &+ DRA(i,3)*DRA(i,3)

    grad_n = sqrt(GAA+GBB+2*GAB) !2.0d0*GB!**(1/2)

    s = abs(grad_n)/(2.0d0*(3.0d0*(PI**2.0d0))**(1.0d0/3.0d0)
    $*n**(4.0d0/3.0d0))

    TauW = (grad_n**2.0d0)/(8.0*n)

    Tau_unif = (3.0/10.0)*(3.0*(PI**2.0d0))**(2.0d0/3.0d0)
    $*(n**(5.0d0/3.0d0))

    Tau = TB

    alpha1 = (Tau - TauW)/Tau_unif
    x = mu_ak*(s**2.0d0) * ( 1.d0 + ( (b4*(s**2.d0))/mu_ak )
    $* exp((-abs(b4)*(s**2.d0))/mu_ak) ) + (b1*(s**2.d0) + b2
    $* (1.d0 - alpha1)*exp(-b3*(1.d0 - alpha1)**2.d0) )**2.d0

    x1 = 1.d0 - alpha1
    x2 = alpha1 - 1.d0

        !Basic Heaviside step function code implementation
        if(x1 < 0.d0) then
            theta1 = 0.d0
            theta2 = 1.d0
        else if(x1 > 0.d0) then
            theta1 = 1.d0
            theta2 = 0.d0
        else
            theta1 = 0.5d0
            theta2 = 0.5d0
        end if

    h1x = 1.d0 + k1 - ( k1 / (1.d0 + (x/k1)) )

    !Note the author has a positive (1.d0/2.d0) in his code
    gx = 1.d0 - exp(-a1*(s**(-1.0d0/2.0d0)))

    fx1 = exp( (-c1x*alpha1)/(1.d0-alpha1 ) )*theta1
```

```
47
48          if(fx1 /= fx1) then !Handles NaN issues
49              fx1 = 0.d0
50          end if
51
52      fx2 = -dx*exp( c2x/(1.d0-alpha1) )*theta2
53
54          if(fx2 /= fx2) then !Handles NaN issues
55              fx2 = 0.d0
56          end if
57
58      fx = fx1 + fx2
59
60      Fex = (h1x + fx * (h0x - h1x) )*gx
61
62      ex_unif = -(3.0d0/(4.0d0*PI))*(3.0d0*(PI**2.d0)*n)**(1.d0/3.d0)
63      exc = ex_unif * n
64
65      !Numerical Integration sum
66      F(i) = F(i) + exc*Fex
67
68  end do
69
```

3.4 Results

The aug-cc-pVTZ basis set was used for the Ne, Ar, and Kr atoms. This basis set was chosen due to its "heaviness." The more terms in the basis set, the more accurate it tends to be. For the Xe atom, the DZVP basis set was used since there is no aug-cc-pVTZ currently available for Xe. Results from the author's study are shown in Table 1 and data from implementation of the author's study is captured in Table 2.

Table 1: The author's results from the supplemental material[62].

	Ne	Ar	Kr	Xe
E_x	-12.108	-30.188	-93.890	-179.200
E_c	-0.391	-0.723	-1.850	-3.000
E_{xc}	12.499	-30.911	-95.74	-182.2

Table 2: Results from in-house implementation of SCAN and author's implementation.

Exchange Energy, E_x (Hartree)		
Atom	xTron Implemented Subroutine	Author's Code
Ne	-12.1582	-12.1582
Ar	-30.2618	-30.2618
Kr	-94.0691	-94.0691
Xe	-179.095	-179.095

3.5 Validation

The previous plan was to compared our findings of an already existing software package such as NWChem. Instead, for the first validation, results are compared directly with the author's supplementary material [62]. Also, the author's code/subroutine was implemented into the xTron software for testing. The results were validated by comparing those produced by the author's code with my subroutine implementation of the density functional. Numerical integration used quadrature grids, Lebedev for the angular component and Euler-MacLaurin for the radial component. The number of radial grids used was 128 and 302 angular grids were used shown in Figure 4.

3.6 Tools

MATLAB R2016a was only used to prototype the solution on a Macbook Pro retina laptop running the Mac OS X El Capitan (10.11.6) Operating system. Programming of the subroutine was done in Fortran 77/90 using the Intel (16.0.2) compiler. Unfortunately, the High Performance Computing (HPC) resource, Darter, was decommissioned and a scaling study as well as a speed study comparing compilers was not

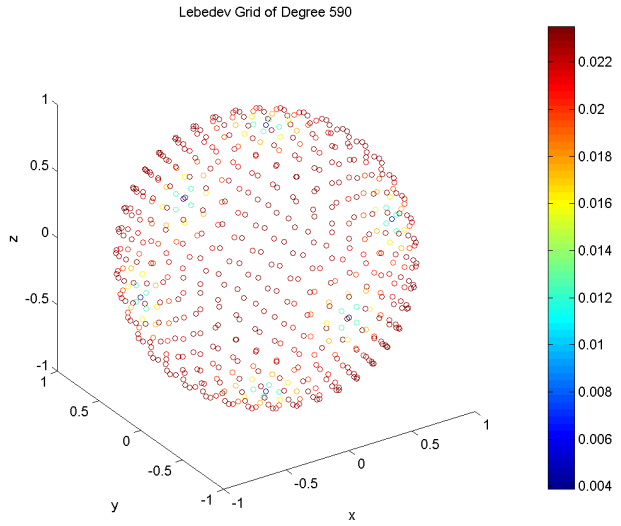

Figure 4: A typical Lebedev sphere with 590 points[52], representing the geometry of an atomic system.

possible. All work was done on kong-srv (8 physical processors, 8 virtual processors for hyperthreading).

3.7 Conclusion

Now knowing the results of strongly constrained and appropriately normed semilocal density functional for these noble gases, we can take this knowledge and use it to create better density functionals. Currently, we have created and implemented Kong-Proynov14/Becke13 which will be improved upon significantly in the near future. This study showed two things: 1) other density functionals can be implemented seemlessly into the xTron code making it possible to benchmark many other functionals against KP16/B13 and 2) it is possible to improve the accuracy of KP16/B13.

4 METHODOLOGY OF STUDY 2

4.1 KP16/B13 Density Functional

The famous functional Becke'13 (B13) is a general purpose density functional theory (DFT) created by Axel Becke with the intention of solving strongly correlated molecules. The Kong-Proynov'16/B13 (KP16/B13) functional is an alteration of the B13 functional that approaches the treatment of the correlation kinetic term through modeling the adiabatic connection. KP16/B13 contains fewer parameters than B13[72]. KP16/B13 is based in Kohn-Sham DFT and also uses a 100% exact exchange. The Kong-Proynov16/Becke13 (KP16/B13) functional calculates the strong correlation well, which is why there is merit in using it to solve for odd electron populations in systems.

The ND correlation phenomenon is described by a linear combination of two terms: one static, an adjustment of the B05 ND correlation and the other SD (strong correlation) involving covalent dissociation bounds. A description of SD is given by KP16/B13 based on B13's strong correlation model having a foundation on its static correlation potential and an extra correction of the fractional spin error. This is partly the reason why these functionals are shown to produce more accurate results for extremely strongly correlated systems than their contemporary counterparts[72].

The following is the nondynamic correlation energy where u is the B13 static correlation potential energy density with an add-on of fractional-spin correction term to a fractional spin error correction and q is a real-space function that includes the correlation based kinetic energy contribution which is based on a local AC model bounded be 1/2 and 1. Nondynamic correlation is weak around $q = 1/2$ and very strong at q around 2.

$$E_c^{ND} = \int q(r)u(r)dr^3 \tag{66}$$

The KP16/B13 functional uses a single term to address the dissociation limit along with a correction for the fractional spin error at this limit. The adiabatic connection-coupling (AC) method is used to calculate the correlation energy portion of the functional. The combination of this functional with an AC-coupling strength integrated dynamic correlation, enacted with SCF, produces a general correlation functional for thermochemistry and strongly correlated systems based on single-determinant representation[35].

$$E_c = \int_0^1 W_\lambda^c d\lambda \tag{67}$$

Only a few empirical parameters are used in KP16/B13 in order to describe the nondynamic/strong correlation and calculations of atomization energies as well as singlet-triplet energy splittings are produced with very little error cancelation. KP16/B13 is also able to take advantage of several well-known exact scaling relations for correlation fuctionals[35].

4.2 The Minnesota Dataset Systems

The M06 has been developed by Donald Truhlar's group at the University of Minnesota group. It is regarded as one of the best theoretical chemistry databases overall.

4.3 Single-Reference Main-Group Nonmetal Bond Energies (SR-MGN-BE107)

This data set is the single-reference main-group non-metal bond energies. The geometries used are QCISD/MG3. This set is composed of 95 single-reference nonmetal molecules from the Minnesota group's SRNM95 subset and all main group single-reference molecules from the MGAE109/11 set. The table of these results is much too large to display in this document.

4.4 Computational Experiments

Solely using xTron software for our main runs: KP16/B13 functional and G3LARGE basis set for the geometries provided by the Truhlar's supplementary material. Our results were compared against SCAN, B3LYP, MN06, ωB97x, and B13 functionals using the G3LargeXP basis set with DIIS (Direct Inversion of Iterative Sub-space)[58] and GDM when convergence is needed.

We suspect that depending on how the KP16/B13 functional performs on calculating the atomization energy (AE) of the Minnesota set of organic molecules, that would give a good indication on how well the calculations for the density of atomic population of localized electrons (APELE) in PAHs would do. This choice of benchmarking is particularly appealing because the Minnesota set is the gold standard of overall performance density functional performance on a handpicked, diverse sets of chemical systems.

4.5 Seven Hydrocarbons HC7/11

Ranging from octane isomers to hexane, these are several systems that are comparable to some PAHs that we will be studying. The species involved are sensitive to medium-range correlation energy. This Minnesota set is the joining of the HC5 database in addition to two isodesmic reactions, adamantane and bicycle [2.2.2]octane, which were classified as difficult cases by the author Grimme[54].

4.6 Computational Details

4.6.1 HC7/11 Study

The MN15 database contains 30 subsets and two were chosen for this study. The majority of the sets were excluded since we only need at most two to prove our point. The basis set used in all calculations is G3LargeXP. The numerical grid is an atom-centered unpruned ultrafine grid with 128 radial and 302 angular points per shell within Becke's relative weights integration scheme. All calculations are done with SCF with direct inversion in the iterative subspace (DIIS) and/or generalized direct minimization (GDM) SCF convergence schemes[72].

4.7 Benchmarking Results of HC7/11 and SR-MGN-BE107

The main feature of a random, unknown, measurable quantity is how much it changes. Enough priority should be given to quantifying how it varies[12]. There are three statistical quantities of significance when benchmarking a density functional: the Mean Unsigned Deviation (*MUD*), Mean Signed Deviation (*MSD*), and Maximum Deviation (*MaxD*).

The *MUD* and the *MSD* is calculated the following following respectively.

$$MUD = \frac{\sum |x_i - \text{referencevalue}|}{\text{total}\#} \tag{68}$$

$$MSD = \frac{1}{n}\sum_{i=1}^{n} \bar{x} - x_i \tag{69}$$

Where x_i is the calculated value and $\bar{x}$ is the mean of the data set. The maximum deviation is the largest of $\mid \bar{x} - x \mid$ values. The MSD encapsulates how well a set of data matches the theoretical results. The MUD, also known as the mean absolute deviation, is the average distance between each data point and the mean.

Since KP16/B13 results are adequate on the SR-MGN-BE107 and HC7/11 sets in comparison with the other functionals, then the justification exists to move forward with studies of other larger organic systems, namely PAHs.

The first two entries in HC7 are isomerization energies of the systems $(CH)_{12}$ isomer 1, 22, and 31, while the third is energy of reaction of the system called octane isomerization. Data entries four through seven are energies of reaction for similar reactions[80].

For this database we used the G3LargeXP basis set. All calculations are done with self-consistent-field (SCF) with DIIS [58] and/or generalized direct minimization (GDM) [70] SCF convergence schemes.

Functionals	SCAN	B3LYP	M06	ωB97x	B13	KP16/B13
HC7/11						
MUD	6.67	-31.23	2.29	7.21	26.99	15.11
MSD%	0.67	-1.00	0.90	0.58	-1.00	-1.00
MaxD	22.87	-30.27	5.67	16.16	-60.31	-31.23

Table 3: Statistical summary performance of several DFT methods for the hydrocarbon data set. The deviations are in kcal/mol. The best performing functional for this set is displayed in the last column.

4.8 Conclusion

The results of the benchmarking study are consistent with the other functionals regarding the Minnesota set. In general, the hydrocarbon and organic molecule results are consistent with what other authors have calculated with other computational chemistry methods. Results of KP16/B13 calculations on hydrocarbons show that similar systems such as PAHs would be good potential systems fit for studying with the APELE method.

5 METHODOLOGY OF STUDY 3

The Configuration Interaction (CI) study that Lischka et al presented in their paper, titled Polyradical Character of Triangular Non-Kekule Structures, Zethrenes, p-Quinodimethane-Linked Bisphenalenyl, and the Clar Goblet in Comparison: An Extended Multireference Study, only used 6 electrons! They exploited symmetry and scaled the answers for the other side of the systems used.

5.1 Systems Studied

Adding benzene rings in a few triangular ways can result in some π-conjugated phenalenyl products like triangulene, π-extended triangulene, and larger systems[77][78]. These molecules are grouped as polynuclear and benzenoid in nature having some unpaired electrons[16].

5.2 Non-Kekule Triangular Molecules, Systems 1-3

Triangulene ((IUPAC name: 4H,8H-dibenzo-[cd,mn]pyrene-4,8-diyl)), also known as, clar's hydrocarbon has been studied since 1941. It is strange in that it is the most elementary non-Kekule PNB (polynuclear benzenoid) for which no Kekule formulas

can be permitted to have. Two carbons do not contribute to the double bonding of the system which increases the chances of having an open-shell structure[29].

Overall, the general consensus is that you see less odd electron density in the center of the molecule for all three cases. Therefore, stronger bonds happen due to the changing of the geometry.

5.2.1 System 1 - Phenalenyl

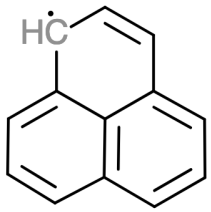

Figure 5: Phenalenyl radical

Similar to several other PAHs, phenalene, also known as 1H-Phenalene, is a chemical that polutes Earth's atmosphere. It is the product of the combustion of fossil fuels and the parent compound for phosphaphenalenes and one of the most fundamental delocalized neutral radicals[47]. The radical version of this system is called phenalenyl and is shown in Figure 5. Molecular orbital degeneracy in phenalenyls partially provide a gain in electric current capacity in molecular batteries[47].

5.2.2 System 2 - Triangulene

The tiniest triplet PBN that is in the ground state is the diradical triangulene, shown in Figure 6, which was discovered in 1953. Triangulene has the chemical formula $C_{22}H_{12}$, with an even number of carbons, was first theorized by Czech chemist Eric

Clar. This makes it impossible to draw Kekule-style resonant structures for the entire chemical system since you have two unpaired electrons left-over in the valence shell. Around 2016 to 2017 this chemical system was first synthesized successfully by David Fox, et al and IBM[53].

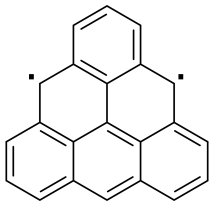

Figure 6: Triangulene, courtesy of Wikipedia

Dihydrotriangulene is very difficult to synthesize. When completed, it produces two isomers of dihydrotriangulene that scientists can place on a xeon or copper base. Experimentalists used scannning tunneling microscopes (STM) and atomic force microscopy (AFM) to take away any additional hydrogens, giving it a stable lifetime of four days.

5.2.3 System 3 - π-extended triangulene

This π-extended radical, if looking purely at the geometry can be viewed as a triangle cutout of graphene. In the field they are called open-shell graphene fragments and can be seen in Figure 7. An interesting property is that when examining the spins of these and other π-extended molecules, we see ferromagnetic properties[47].

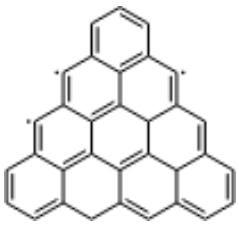

Figure 7: π-extended triangulene

5.3 Heptezethrenes, Systems 4-6

The Z-shaped PAHs, heptazethrenes, were synthesized first by experimentalists from chrysene-2,8-dicarboxylic dichloride and then condensed, cyclized, processed via decarboxylization and a reduction reaction, and then dehydrogenated[27].

5.3.1 System 4 - Heptazethrene

Heptazethrene is a PAH with seven (greek word hepta) benzene rings bonded to create the geometry. A picture of heptazathrene can be seen in Figure 8. It is also a basis hydrocarbon and very similar in relation to dibenzoheptazethrene which is discussed next[32].

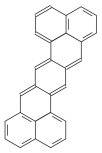

Figure 8: Heptazethrene

5.3.2 System 5 - Dibenzoheptazethrene

The prefix di means two. Joining two benzene rings to the upper left and lower right corner of heptazethrene and that will yield dibenzoheptazethrene.

5.3.3 System 6 - 5,6:13,14-Dibenzoheptazethrene

The quinoidal geometry of 5,6:13-dibenzoheptazethrene consist of two aromatic sextets. More can be present with a maximum of five for the dibenzoheptazethrene general structure. Many chemists and physicists anticipate that an increase in aromatic sextets for 5,6:13,14-dibenzoheptazethrene will make this molecule stable in the biradical resonating geometry[67].

5.4 Systems 7-8

Geometries of these systems by default are twisted. Their optimized geometry, however is flat and much easier to deal with for purposes of calculating their stable energies.

5.4.1 System 7 - p-Quinodimethane-linked Bisphenalenyl

This structure is composed by a resonance form of quinoid, diradical, and clar's sextet ring. The ring causes its unstability[17].

5.4.2 System 8 - Clar Goblet

Clar's goblet, $C_{38}H_{18}$, is a concealed diradical benzenoid. It forms by combining two benzo[cd]pyrene monoradicals ($C_{19}H_{11}$)[19].

5.5 Nakano Systems 1 - 8

These systems are variations of NDPL and IDPL: dicyclopenta[b;g]naphtha-lene[1,2,3-cd;6,7,8-c'd']diphenalene(NDPL) and s-indaceno[1,2,3-cd;5,6,7-c'd']diphenalene(IDPL).

Two-photon absorption (TPA) was measured by Kamada et al of singlet diradical hydrocarbons with IDPL and NDPL diphenalenyl radicals. These were sythesized by Kubo et al and were measured to have a very large cross section, over 1,000 nm[50].

5.5.1 NDPL

Not much is known about this newly sythesized system. This is uncharted territory for the field. NDPL is known more formally as dicyclopenta[b;g]naphtha-lene[1,2,3-cd;6,7,8-c'd']diphenalene.

5.5.2 IDPL

The IDPL system is a thermally stable diradicaloid due to both resonance structure forms: quinoid and benzenoid. "Namely, the recovery of aromaticity in the central benzene ring in s-indacene part of IDPL leads to the diradical structures."

"The IDPL is known to make a needle-like one-dimensional (1D) crystal, where the monomer is arranged in a slipped stack form." The system shows a very short $\pi - \pi$ distance of 3.137 Angstroms. This is less than a representative van der Waals distance of 3.4 Angstroms. It also has large conductivity and also a large absorption peak shifted to the low-energy region[49]. This is another newly synthesized s-indaceno[1,2,3-cd;5,6,7-c'd']diphenalene(IDPL)

5.6 Results

5.6.1 Triangular Non-Kekule Structures

For all three of the following cases, distribution of APELE at edges is alternant and the unpaired density resides only on the starred atoms. Again, Lischka's CI study only used six electrons[16]. They exploited symmetry and scaled the answers for the other sides of the molecular systems. Overall, in our study we see less APELE in

the center of the molecule for all three cases which is consistent with Lischka et al's findings. The number of unpaired electrons, N_U is calculated using the "map" on Chart 1 in the Lishcka article[16].

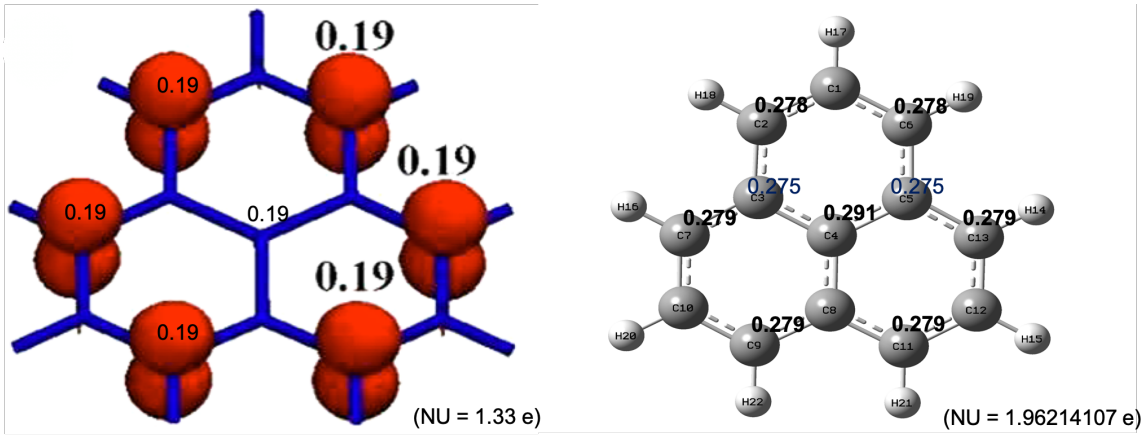

Figure 9: Phenalenyl singlet APELE results using 6-31G basis set.

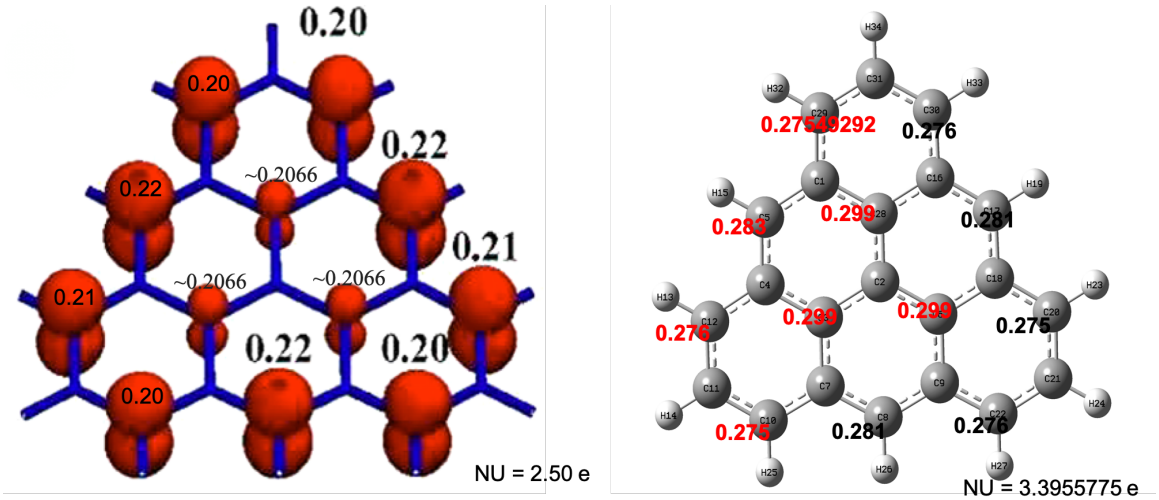

Figure 10: Triangulene singlet APELE results using 6-31G basis set.

In Figure 9, a comparison is made against the data given in the supplemental material by Lischka, et al. Our APELE results are consistent with theirs. Effectively unpaired electrons are delocalized over the whole molecule and reside mainly on the edges of the molecule although Lischka makes clear that the phenalenyl central carbon

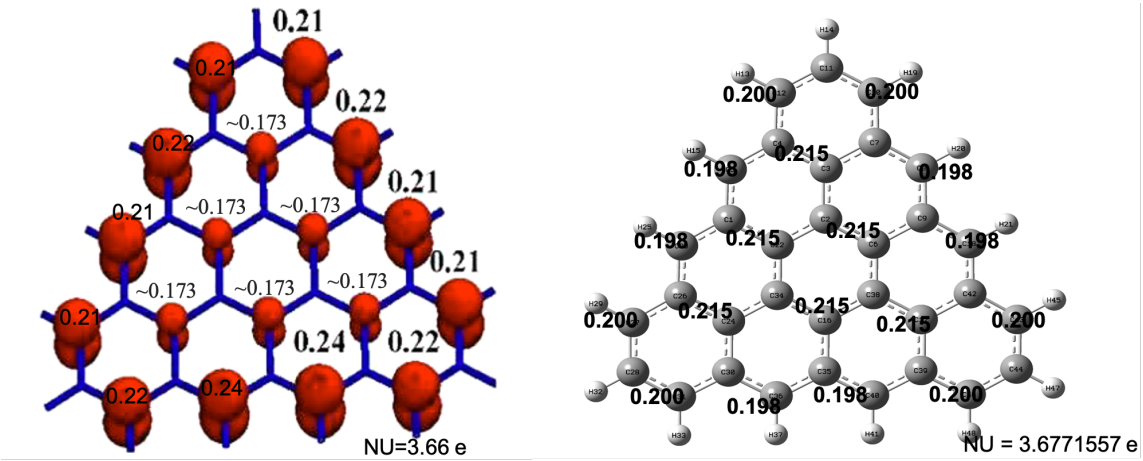

Figure 11: The π-extended triangulene quartet APELE results using 6-31G basis set.

atom does have unpaired electron density.

In triangulene, shown in Figure 10, the results are consistent with Lischka, et al. Electrons are localized over the whole molecule and reside mainly on the edges of the molecule. The variation of the number of unpaired electrons, N_U, is also consistent. This depletion of unpaired density in the central region of the triangle has important consequences on the shape of stacked biradical dimers (convexity). This is readily consistent with the author's results that electrons delocalized over the whole molecule reside mainly on the edges of the molecule.

The π-extended triangulene in Figure 11 shows that the electrons are delocalized over the whole molecule. They reside mainly on the edges of the molecule and concentrations of unpaired electrons are only slightly different from Lischka et al's study in the system. Results are not necessarily consistent as they look to be opposite while electrons are delocalized internally(central).

It is noteworthy that the APELE values, N_U presented in Figure 11, in comparison to Lishcka et al, are larger as compared to the formal open-shell occupation of the high-spin state (1.33 vs 1 for phenalenyl, 2.50 vs 2.0 for triangulene, and 3.66 vs 3.0 for the π-extended triangulene system). Another reason for the differences in results

is that Lishka et al use the Head-Gordon formula for calculations, while APELE is based on the original formula of Yamaguchi et al. Head-Gordon's formula counts all of the unpaired electrons, whereas APELE only counts those electrons that are truly multireference.

One path moving forward to address the inconsistencies would be to try again without Geometry Direct Minimization (GDM). We can also try repeating the calculations with larger basis sets.

5.6.2 Zethrenes

There appears to be radical character distributed over a few positions denoted by arrows shown by Figure 12. The APELE values within the benzene ring connecting the two phenalenyl segments is significant. This is consistent with Lischka's results[16] - radical character distributed over a few positions denoted by arrows.

Figure 13 is where things are slightly different due to the symmetry being different for this system. Inside the green circle going from left to right denotes an increase in concentration of APELE. The radical character is mostly distributed over several positions. This happens to be consistent with Lischka et al's results that the radical character is mostly distributed over a few positions.

Figure 14 is also consistent with the author's results - the radical character is mostly distributed over a few positions. Note, however, that the C15 (top middle, Figure 14 on the right at C17) atom has a slightly higher unpaired electron density than C12 (Figure 14 on the right C29).

5.6.3 p-Quinodimethane-Linked Bisphenalenyl and Clar Goblet

Figure 15 is consistent with the Lischka's results and maybe even better. Here, the biradical configuration of the central benzene ring has aromatic character. This should

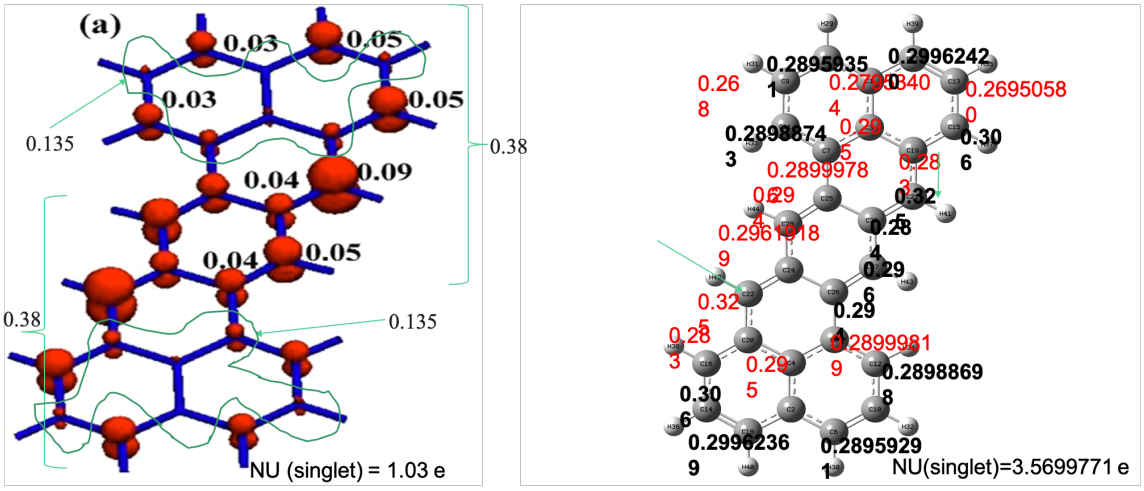

Figure 12: Heptazethrene singlet APELE results using 6-31G set

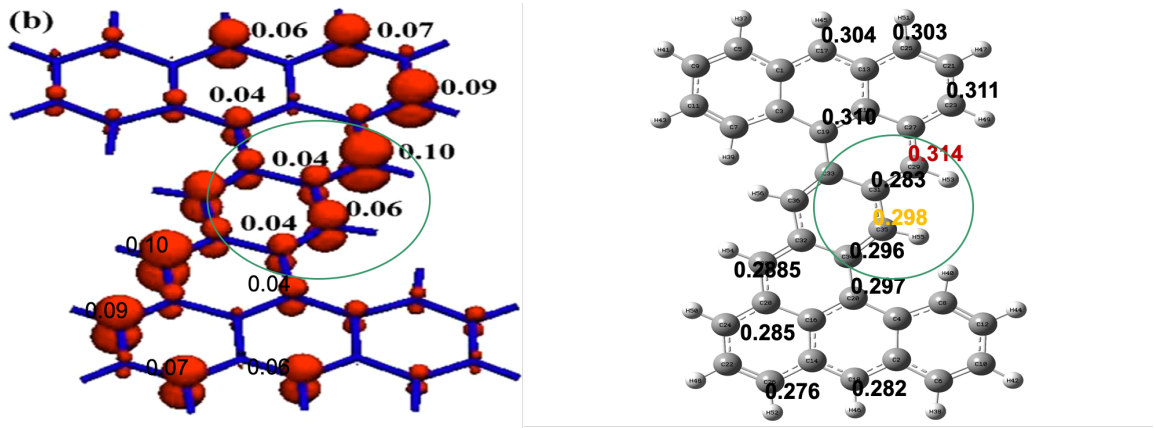

Figure 13: Dibenzoheptazethrene singlet APELE results using 6-31G set.

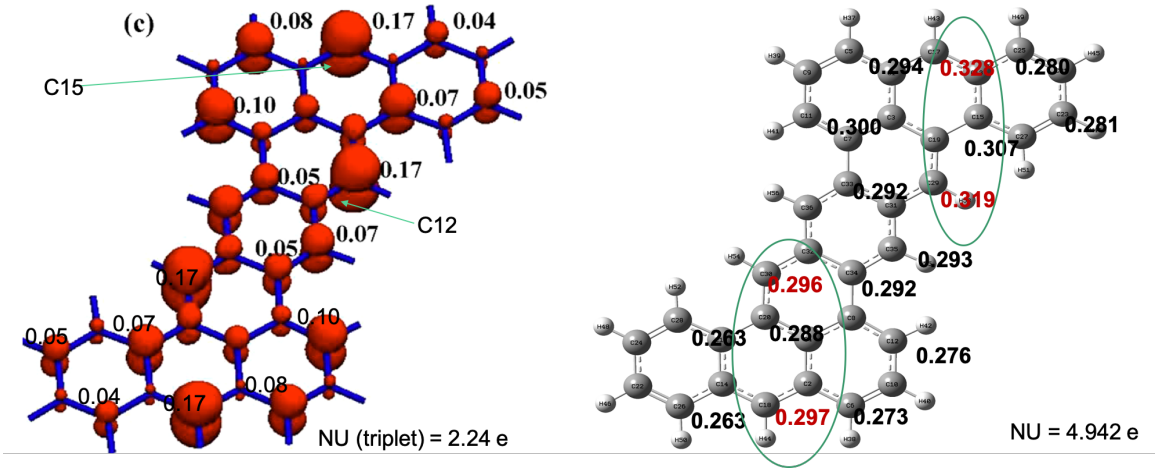

Figure 14: The 5,6:13,14-dibenzoheptazethrene singlet APELE results using 6-31G basis set.

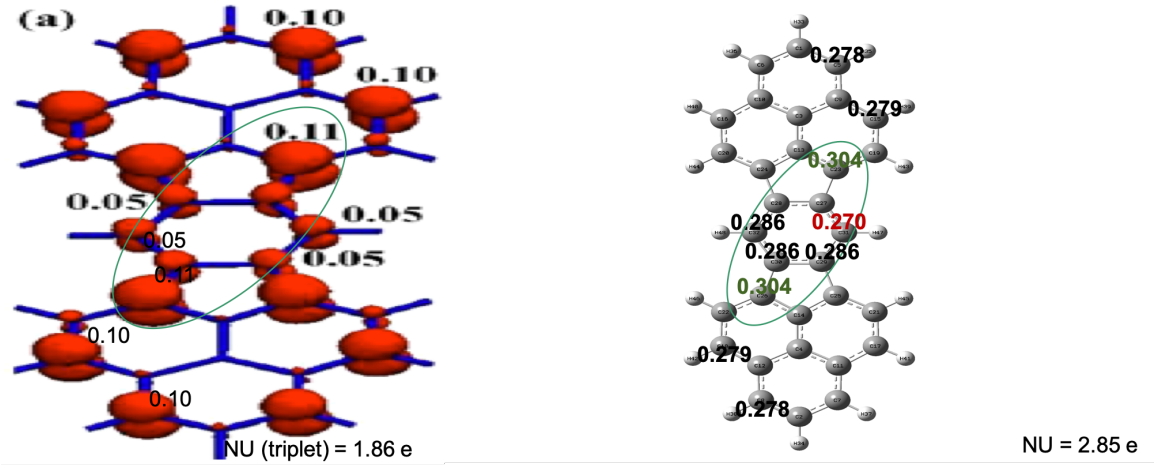

Figure 15: The p-quinodimethane-linked bisphenalenyl singlet APELE results using the 6-31G basis set

lead us to believe that structure 7 will also possess significant biradical character[16].

In Figure 16, it appears that the results are not consistent with Lischka's. A repeat of the calculations with a different basis set such as 6-31G* would be worth investigating further.

Other scientists exploring DFT with graphene-like structures report that a large amount of issues dealing with DFT software are due to delocalization error or something of that nature[14]. Static correlation error of density functionals is basically an inconsistency in the fractional spins[30]. Yang et al go on to suggest that there is a lot of evidence showing that inside the deviations is a built-in delocalization error in aromatic compared to nonaromatic isomerization with respect to the delocalization of the fractional charges[14].

One reason for the APELE numbers showing a different trend from Lichka et al for some structures such as the triangulene triplet, π-ext-triangulene) is the formula the author uses. Lishcka et al measure all of the unpaired electrons including true spin-polarization in open shells and effectively unpaired electrons due to the nondynamic correlation, also known as the effective electron localization. The former effects are in

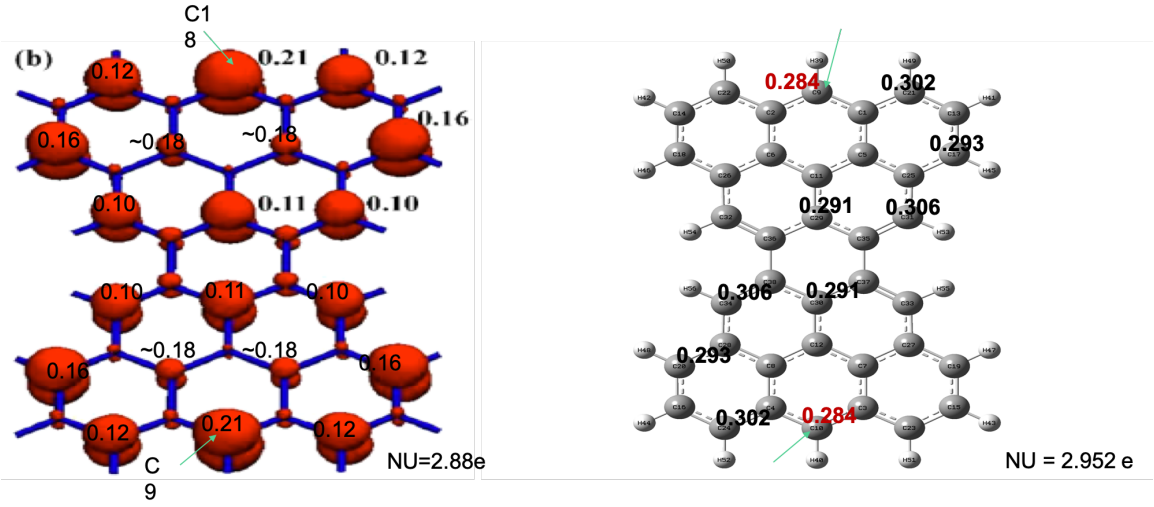

Figure 16: Clar goblet singlet APELE results using the 6-31G basis set.

open-shell systems such as in a radical system with multiplicity larger than one. The APELE method only measures those effects that result from nondynamic correlation.

True radical chemical systems have unpaired electrons. For example, a hydrogen atom is technically radical because it has one unpaired electron. However, this electron lacks non-dynamic correlation. Lischka et al's method includes this effect in their calculations, while our method, APELE, does not.

5.6.4 Non-conjugated/Conjugated Kekule Biradicals

Kubo et al of this paper [37] lists these eight types. There are eight geometries in the supplemental material that do not have any of what is previously listed such as nitroxides, etc. According to the article, the author synthesized these systems and then stripped off these groups that were attached. By doing so, they all had a slightly modified geometry which they were able to accurately obtain through X-ray crystallography, NMR and other techniques, namely ORTEP.

In the supplemental material[37] of Singlet Biradical Character of Phenalenyl-

Based Kekule Hydrocarbon with Napthoquinoid Structure, there are eight geometries given.

Regarding Figure 17 and 18, Systems 1 and 2, there appears to be vertical symmetry with the APELE N_U values of all figures. The central benzene rings appear to contain aromatic character. There is unpaired character mostly located at the zigzag edges and significant amount of unpaired density located on the connecting rings relative to total APELE N_U.

In Figure 19, the central benzene rings also contain aromatic character. As with the figures mentioned previously, there is unpaired aromatic character located at the zigzag edges. In Figure 20 and 21, there is mostly vertical and horizontal symmetry in unpaired electron density. The APELE values are significant at the upper middle and lower middle outer locations, similar to the APELE value locations of the clar goblet in Lischka's study. Also, the base triangulene section of those molecules appear to have aromatic character due to the high APELE value. In Figure 22, there is also vertical and horizontal symmetry. The aromaticity also appears in the same general location as the previously mentioned figures. In Figure 23, there is more aromaticity exhibited at the top and bottom of the system and consistently on the outer zig-zag edges. In Figure 24, there appears to be a concentration of aromaticity on the outer top and bottom 1/3 area of the system. This is consistent with the similar geometries of the systems in Lischka's study as well as what is reported by Molcanov and Kojic-Prodic[46].

The compounds show inter- and intramolecular interaction strength between two unpaired electrons. These inter- and intramolecular covalent characteristics cause π-π orbitals to become significantly close. This results in wide valence and conduction

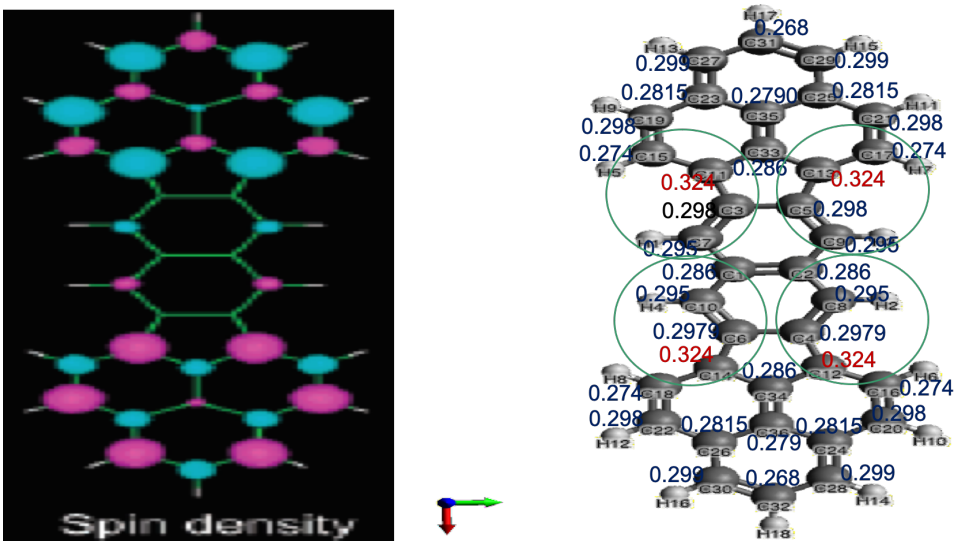

Figure 17: System1 (singlet) NDPL APELE results: D2H HF for initial guess and then KP16/B13 using 6-31G** basis set.

bands in the system[28]. "Thus, phenalenyl-based singlet biradicals will open up a new avenue for highly delocalized 1D electronic structures."[38]

These singlet biradical molecules give underlying understanding, further showing that intermediate bonding interaction of electron pairs can give rise to intra- and intermolecular bonding[61].

5.7 Computational Experiments

In comparison to the previous study, these calculations use the xTron software. Main runs also use the KP16/B13 density functional and APELE. The functionals B3LYP and BLYP are also used to verify energy results. We use the 6-31G, 6-31G*, 6-31G**, and occasionally the G3LARGE basis sets with DIIS or GDM for help with convergence.

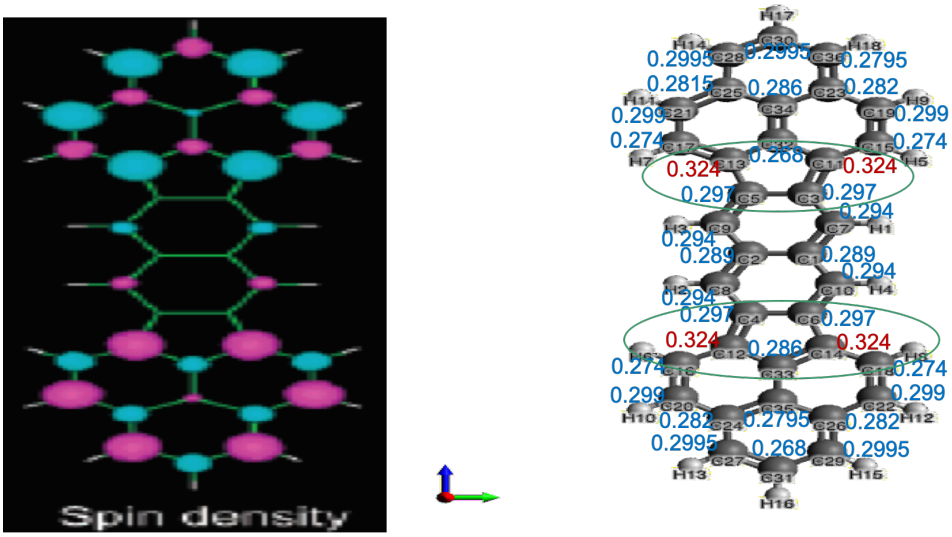

Figure 18: System2 (singlet) NDPL biradical APELE results: D2H Broken Symmetry, HF for initial guess and then KP16/B13 using 6-31G** basis set.

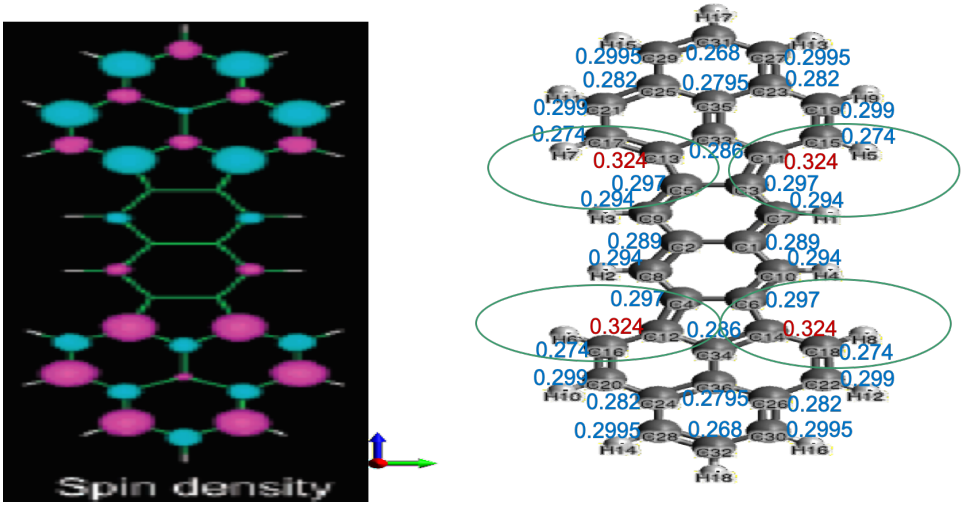

Figure 19: System3 (singlet) NDPL ground state APELE results: D2H Broken Symmetry, HF for initial guess and then KP16/B13 using 6-31G** basis set.

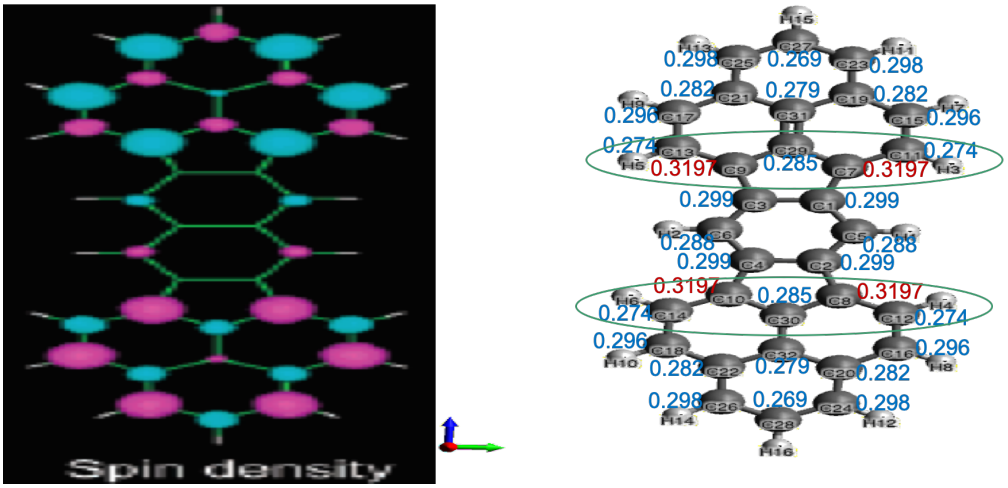

Figure 20: System4 (singlet) IDPL ground state APELE results: D2H Broken Symmetry, HF for initial guess and then KP16/B13 using 6-31G** basis set.

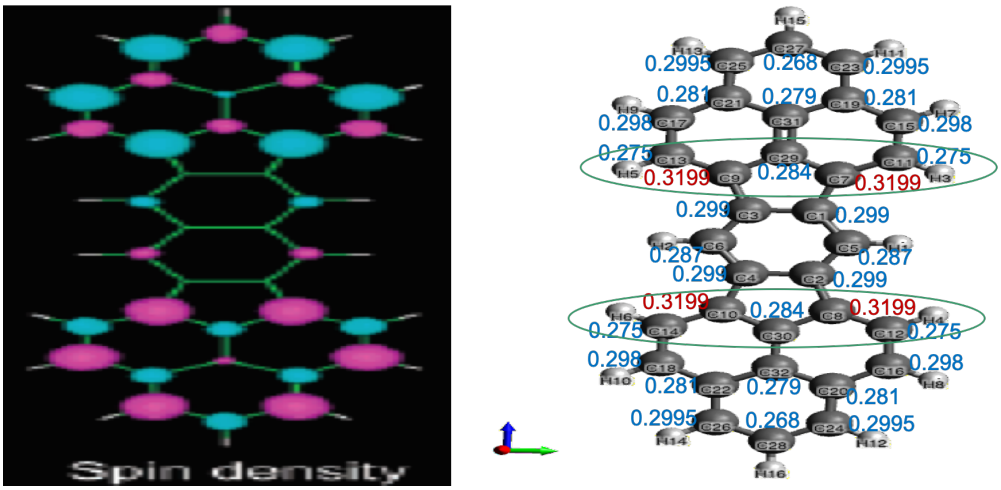

Figure 21: System5 (singlet) IDPL ground state APELE results: D2H Broken Symmetry, HF for initial guess and then KP16/B13 using 6-31G** basis set.

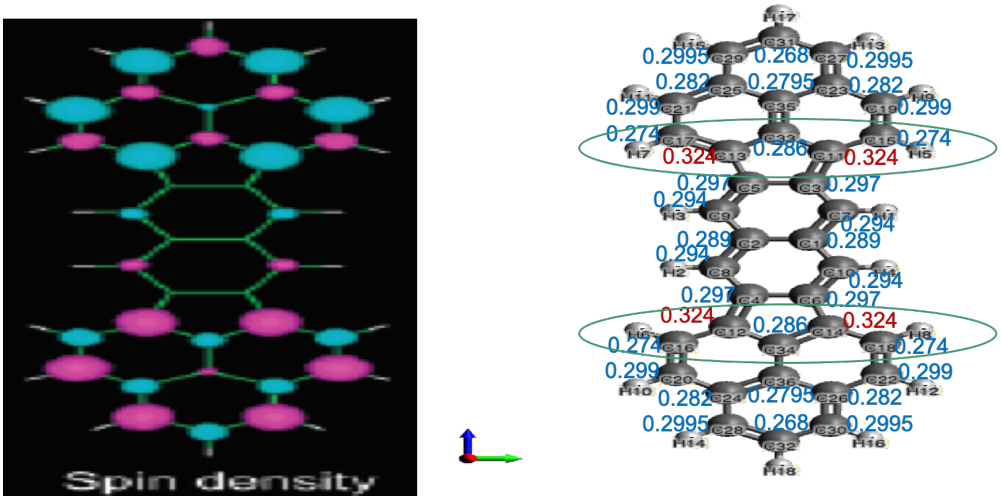

Figure 22: System6 (singlet) IDPL ground state APELE results: D2H Broken Symmetry, HF for initial guess and then using KP16/B13 6-31G** basis set.

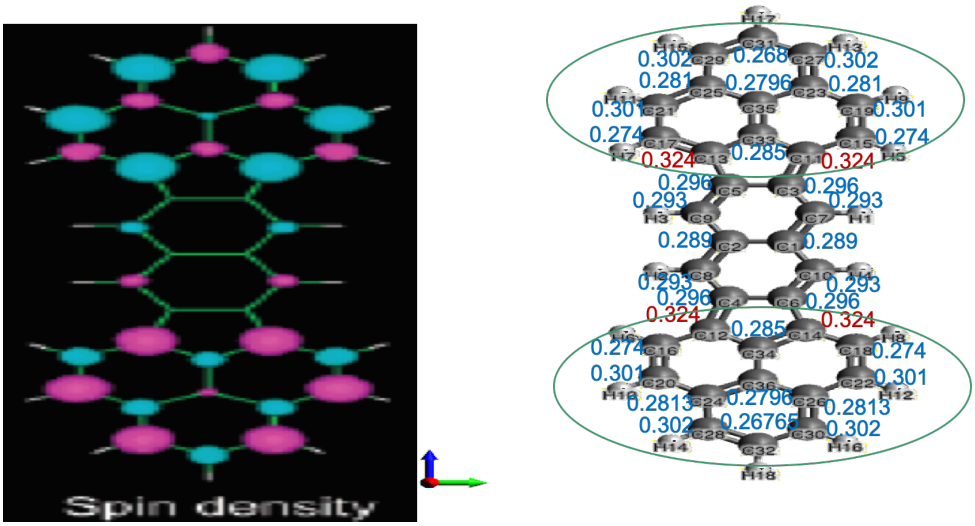

Figure 23: System7 (singlet) IDPL ground state APELE results: D2H Broken Symmetry, HF for initial guess and then using KP16/B13 6-31G** basis set.

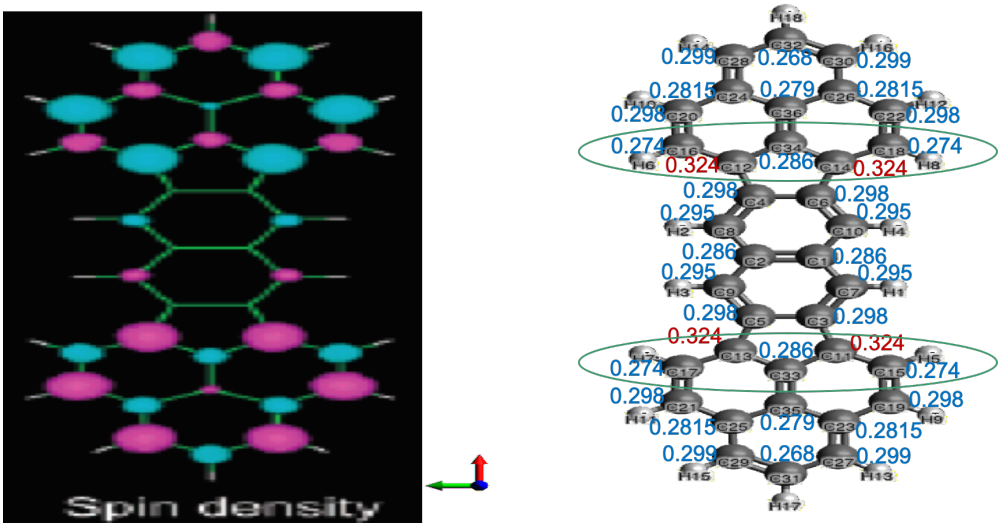

Figure 24: System8 (singlet) IDPL ground state APELE results: D2H Broken Symmetry, HF for initial guess and then KP16/B13 6-31G** basis set.

5.8 Computational Details

The in house software package xTron is used for these calculations. The xTron package was developed in C++ and Fortran with an object-oriented design. It is primarily used to calculate SCF energy and also APELE populations. All calculations, which are shown in Table 3, are done using self-consistent-field (SCF) with DIIS. The xTron software supports automatic threading capability via Intel's Thread Building Blocks (TBB) parallel library for high performance computing capability.

5.9 Conclusion

Overall, APELE agrees with Lischka's and Kubo's results better with singlet systems due to APELE accounting for the static correlation. This is not surprising due to the static correlation manifesting greater in calculations in the singlet state. From our singlet-triplet energy calculations, not presented here, we can see that KP16/B13 results do not provide any conclusive evidence that the singlet-triplet splittings show local correlation treatment for heptazethrenes. We do observe as more rings are added

to a PAH structure, the more stable it becomes.

6 METHODOLOGY OF STUDY 4

6.1 C-C Benchmark

Why is the carbon atom the only element that forms long chains? It is positioned right above the silicon atom on the periodic table of elements and has four electrons in its outer shell. The carbon-carbon bond is very strong because the shared electron orbital is a short distance from the nuclear center and the nuclei has a strong attractive force. The typical bond strength of a typical C-C bond is 347-356 kJ/mol, carbon double bond is 611 kJ/mol, and carbon triple bond is 937 kJ/mol. Because two C-C bonds are stronger than one carbon double bond, long carbon chains are more advantageous than those that are shorter[24].

An important characteristic of the symmetric solution of the Schrödinger equation of a diatomic system is the minimum at some finite distance from the nucleus. Therefore, one of the two possible solutions represents a description of the chemical bond. The other positive solution is called the elastic rebound[31].

The symmetric solution to the Schrodinger equation using the wave equation can shed a light on what compounds can be formed using the Pauli exclusion principle. Even though a symmetric function for two atoms containing two electrons would violate Pauli's principle, the solution correctly describes the bond. The symmetric wave function of the two systems have the same quantum numbers, save for spin. This resulting wave function is the physical form of chemical valence.

6.2 C_n Study

The G3LargeXP basis set will be used to calculate singlet states of C_n carbon chains starting with C_2. The xTron software will also be used and produce plots similar to that of Figure 28.

6.3 C-C-* Benchmark Results

The central bond pair C-C has an equal number of carbon atoms on the left and right. For the energy, the binding energy per atom is plotted, $E_{chain} - \Sigma(E_{atom})/N$ as a function of the C-C distance, the latter kept equal along the chain. One question that deserves our attention is: does the energy curve tend to move closer to the zero line with increasing bond length compared with the ΔE curve for C_2?

For the H_n chains[26], for n of approximately 30, the binding energy per H atom is saturated and the curve approaches closely to the zero line at large R, which is much closer than the dissociation curve of H_2. These chains are very strongly correlated systems, so the closer the energy curve is to the zero line, the better the method adjudicates nondynamic correlation. For APELE and bond order calculations it makes sense to show the trend of these values at the two C atoms in the center of the chain with respect to the chain length, shown in Figure 27. The KP16/B13 functional calculates the singlet ground state lower than the triplet state of C_2 as shown in Figure 25 while Figure 26 shows a theoretical comparison.

In the one-dimensional chain, singlet biradical electrons are included in the covalent bonding process. This process is intermolecular as well as intramolecular in nature[5]. Both of these covalent bonding processes are essential in singlet-biradical-based molecular and properties[60].

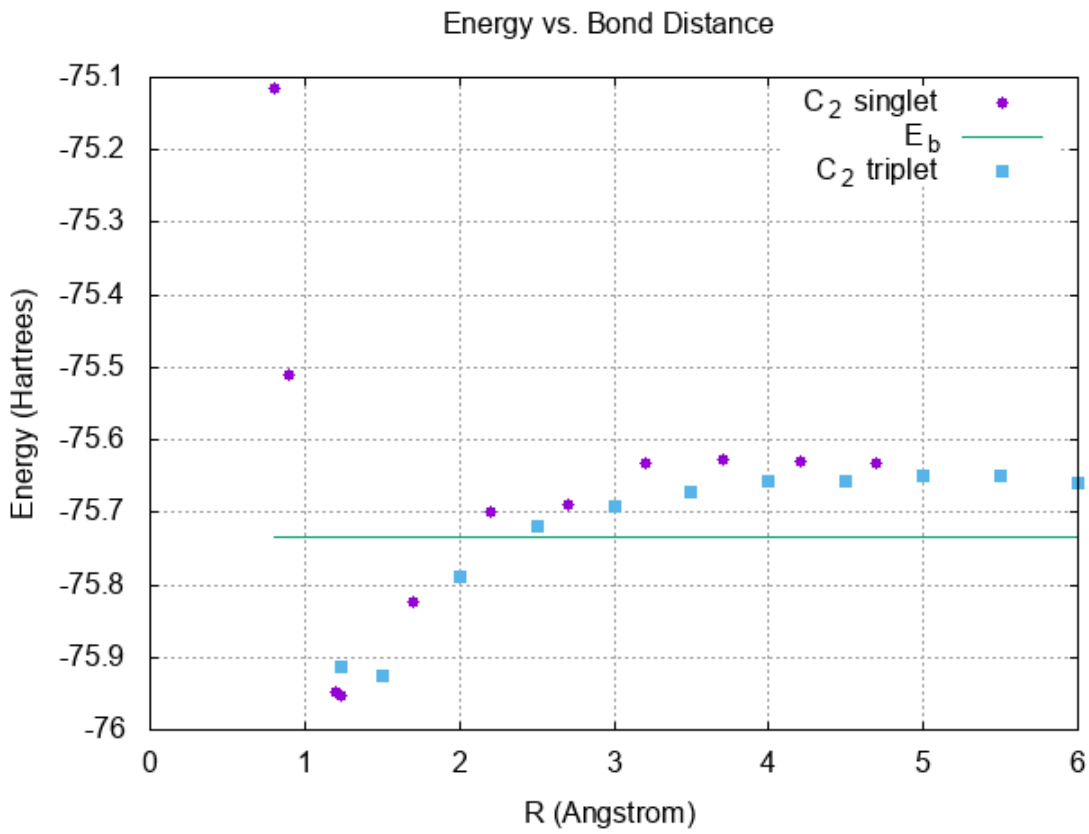

Figure 25: Bond energy of diatomic C_2 with respect to bond distance.

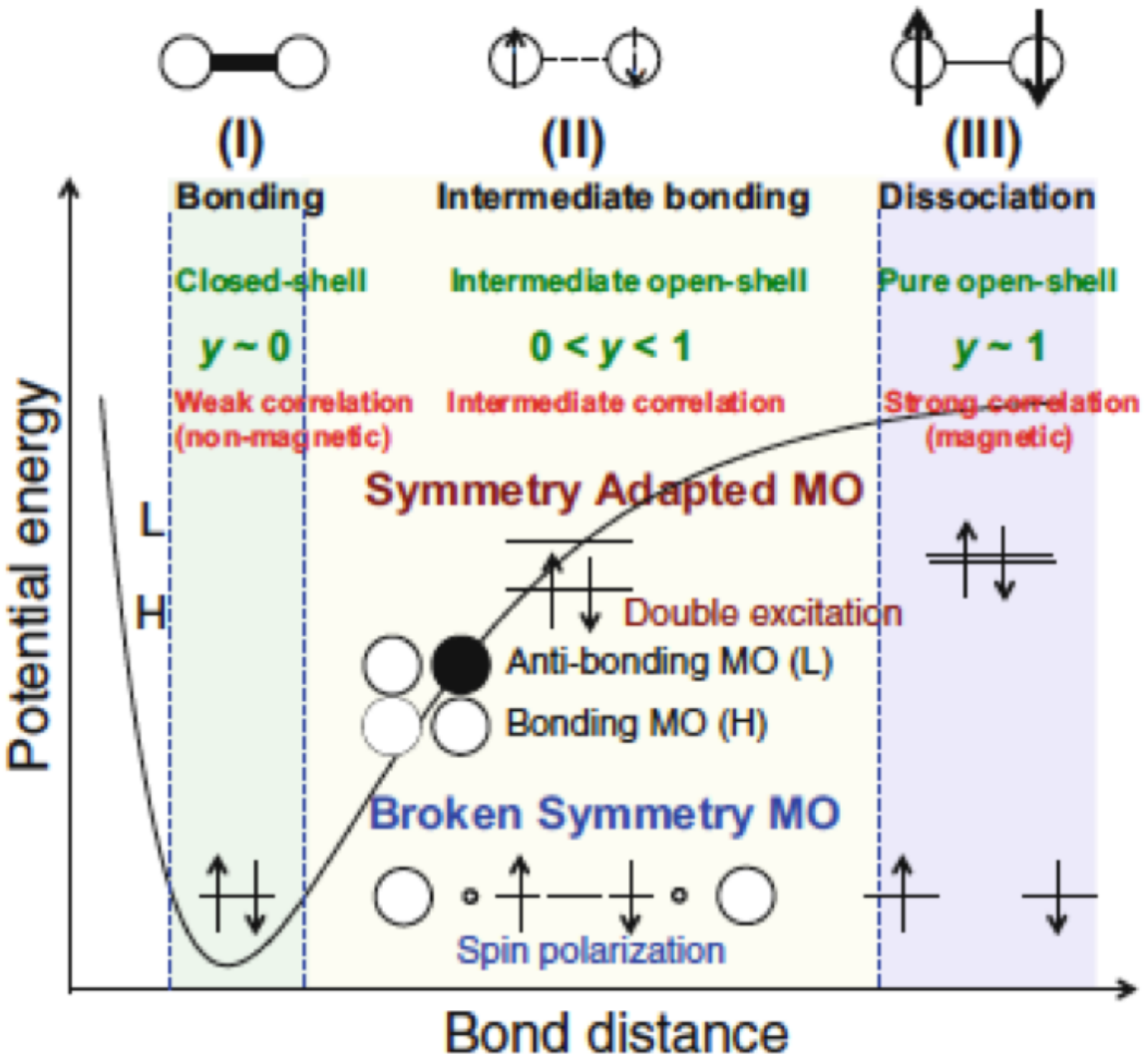

Figure 26: Potential energy versus Bond distance. The figure describes the bond dissociation process of a homodinuclear molecule. The changes of the HOMO and LUMO levels in the symmetry-adapted approach and also the magnetic orbitals for the α and β spins in the broken-symmetry technique are also displayed as a function of bond distance. Physical and chemical definitions of diradical character (y) are also presented in the three regions (I)-(III) of the electronic states in the bond dissociation process[49].

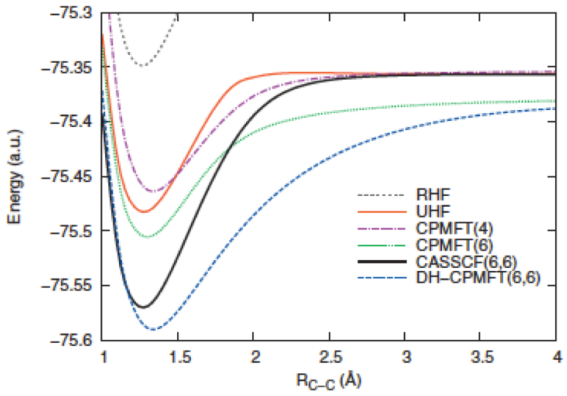

Figure 28: Potential Energy of diatomic C_2 with respect to bond distance using 6-31G basis set and several different theories: RHF, UHF, CPMFT(4), CPMFT(6), CASSCF, DH-CPMFT from an article by Takashi Tsuchimochi and Thomas M. Henderson[69]

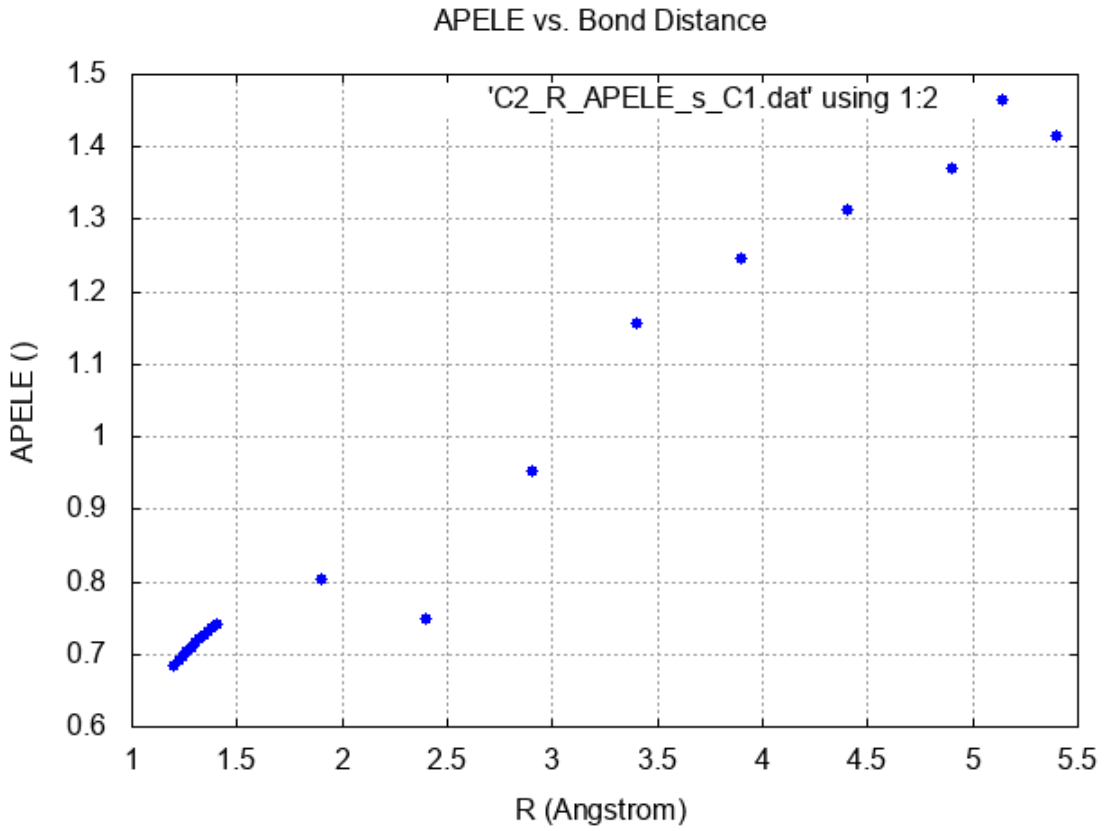

Figure 27: Diatomic C_2 APELE with respect to bond distance.

The C_2 diatomic is very difficult to calculate accurately in terms of its energy

curves. Other authors have benchmarked its energy with respect to bond length which is displayed in Figure 28. It is a diradical molecule of strong nondynamic (ND) correlation. Experimentally, C_2 is a singlet, while most exchange correlations (XCs) give the triplet with lower energy.

6.4 Conclusion

Density functional Becke2005, also known as B05, is a well-known functional that shifted the results in the right direction by giving the singlet value very close to the triplet state, however, the triplet state is slightly lower. Therefore, it is worthwhile to calculate just the singlet C_2 energy curve with KP16/B13 via xTron to see if further improvement over B05 can be achieved. One must be aware of possible severe convergence problems while obtaining the results of the energy curve. Calculating the APELE larger than C_2 and singlet C_n chains would be very interesting. For C_2, APELE results are available in this article [57], with B05 and the results were promising. The equilibrium APELE value is closer to one which indicates the ground state might not be of the diradical type which is in agreement with the conclusions of Sherrill et al. based on FCI analysis. The work of Shaik et al. also suggests a relation between APELE and the correlation corrected bond order based on valence-bond theory that C_2 has an "almost-quadruple" bond multiplicity. All scientists agree that C_2 is a very demanding system, numerically as well.

In the proposed study, most of the data collected should be for large R: up to 6 or 7 angstroms where the asymptotic saturation of the curve occur. Ideally and theoretically, the exact result would result in a curve close to the zero E_b line which is just 2E(C) for full configuration interaction (FCI). With DFT the curve will always be above the zero line for restricted Kohn-Sham (KS) (i.e. no spin-symmetry breaking). The larger the distance of the DFT curve from the true zero line at large R, the bigger

the fractional spin error of the functional. That being said, C_2 is a good test system to assess functionals' fractional spin error[56].

7 SUMMARY AND CONCLUSIONS

This body of work presented demonstrates that APELE can be used to succesfully determine the radical character of PAH systems. Over a dozen molecular systems were studied.

The multi-center bonding contributes to an overlap of large orbitals between molecules. This is in contrast to the electrostatic, polarization, and dispersion forces. Chemical experiments, verified by Kubo et al conclude also that inter- and intramolecular covalent bonding interaction has a significant affect on the electronic structure of the system in the one-dimensional chain.

By extending the volume of the systems in this study, a great multitude of diversity in open-shell character has been confirmed by APELE by comparing the different PAH properties. Analyzing these PAHs with different topological features is now gaining great interest in the field.

We have shown that the APELE method is a useful tool for retrieving reliable information on these compounds. These compounds are very difficult to evaluate experimentally[55] which provides a new way to reliably study these systems.

Our study also shows that singlet biradical character, and to some extent, triplet biradical character in PAHs can be studied in very small systems as well. This is encouraging as it would assist in the field of spintronics and nonlinear optics of

nanographenes[36]

APELE is potentially useful for assessing the radical character of large alternant PAHs, partly due to its computational efficiency. The studies of Kekule and non-Kekule structures in the APELE model helps to qualitatively describe the radical character of alternant PAHs. Our results support previous findings on the increase in radical character with increasing in the volume of the system size. We confirm that the geometry of the rings have a significant affect on the radical character of the alternant PAHs, but not necessarily for the two-dimensional alternant ones[76].

Density functional energy and APELE calculations have been performed on linear cyclic carbon clusters C_n, where the strong correlation is known to be significant[43]. It was communicated in earlier scientific literature that carbon clusters with less than ten atoms have linear ground state structures[42]. There is also evidence to also suggest that linear carbon clusters of up to 16 atoms can be stable in nature[11]. When focusing solely on the C_2 carbon diatomic and its bond distance, APELE breaks down at around the 5.5 Angstrom distance.

With regard to carbon (triplet-state) chains, APELE calculations appear to break down beyond C_7. This linear molecule case has always been difficult in quantum chemistry. Linear molecules have higher symmetry, and as a result, the wave function is easily degenerated in terms of energy. The problem of calculating C_8 and beyond lies in the basis set chosen, which has a linear dependency, therefore the overlap integral matrix cannot be inversed. Going forward, it may be a good idea to use a lighter basis function to avoid the linear dependency. APELE appears to be a powerful tool in investigating larger carbon clusters.

8 PUBLICATIONS

Matthew Wang et al. “Performance of new density functionals of nondynamic correlation on chemical properties”. In: *The Journal of chemical physics* 150.20 (2019), p. 204101

Andrew Adare et al. “ϕ meson production in the forward/backward rapidity region in Cu+ Au collisions at s NN= 200 GeV”. in: *Physical Review C* 93.2 (2016), p. 024904

Justin S Baba, Vijay Koju, and D John. “The impact of absorption coefficient on polarimetric determination of Berry phase based depth resolved characterization of biomedical scattering samples: a polarized Monte Carlo investigation”. In: *Three-Dimensional and Multidimensional Microscopy: Image Acquisition and Processing XXIII*. vol. 9713. International Society for Optics and Photonics. 2016, 97130J

Justin S Baba, V Koju, and D John. “Monte Carlo based investigation of Berry phase for depth resolved characterization of biomedical scattering samples”. In: *Biomedical Applications of Light Scattering IX*. vol. 9333. International Society for Optics and Photonics. 2015, 93330O

Omar ElTayeby et al. “Comparative case study between D3 and highcharts on lustre data visualization”. In: *Visualization and Data Analysis 2014*. Vol. 9017. International Society for Optics and Photonics. 2014, 90170U

9 REFERENCES

[1] Andrew Adare, C Aidala, NN Ajitanand, Y Akiba, R Akimoto, J Alexander, M Alfred, H Al-Ta'ani, KR Andrews, A Angerami, et al. "ϕ meson production in the forward/backward rapidity region in Cu+ Au collisions at s NN= 200 GeV". In: *Physical Review C* 93.2 (2016), p. 024904.

[2] Takeshi Akasaka, Fred Wudl, and Shigeru Nagase. *Chemistry of nanocarbons*. John Wiley & Sons, 2010.

[3] Alexey Akimov and Oleg Prezhdo. "Large-Scale Computations in Chemistry: A Bird's Eye View of a Vibrant Field". In: *Chemical reviews* 115 (Apr. 2015). DOI: 10.1021/cr500524c.

[4] Matthew J. Allen, Vincent C. Tung, and Richard B. Kaner. "Honeycomb Carbon: A Review of Graphene". In: *Chemical Reviews* 110.1 (2010). PMID: 19610631, pp. 132–145. DOI: 10.1021/cr900070d. eprint: https://doi.org/10.1021/cr900070d. URL: https://doi.org/10.1021/cr900070d.

[5] Abduljabar Qassem Alsayoud, Venkateswara Rao Manga, Krishna Muralidharan, Joshua Vita, Stefan Bringuier, Keith Runge, and Pierre Deymier. "Atomistic insights into the effect of polymerization on the thermophysical properties of 2-D C60 molecular solids". In: *Carbon* 133 (2018), pp. 267 –274. ISSN: 0008-6223. DOI: https://doi.org/10.1016/j.carbon.2018.01.044. URL: http://www.sciencedirect.com/science/article/pii/S0008622318300538.

[6] Justin S Baba, V Koju, and D John. "Monte Carlo based investigation of Berry phase for depth resolved characterization of biomedical scattering samples". In: *Biomedical Applications of Light Scattering IX*. Vol. 9333. International Society for Optics and Photonics. 2015, 93330O.

[7] Justin S Baba, Vijay Koju, and D John. "The impact of absorption coefficient on polarimetric determination of Berry phase based depth resolved characterization of biomedical scattering samples: a polarized Monte Carlo investigation". In: *Three-Dimensional and Multidimensional Microscopy: Image Acquisition and Processing XXIII*. Vol. 9713. International Society for Optics and Photonics. 2016, 97130J.

[8] A. D. Becke. "A multicenter numerical integration scheme for polyatomic molecules". In: *The Journal of Chemical Physics* 88.4 (1988), pp. 2547–2553. DOI: 10.1063/1.454033. eprint: https://doi.org/10.1063/1.454033. URL: https://doi.org/10.1063/1.454033.

[9] SF Boys and GB Cook. "Mathematical problems in the complete quantum predictions of chemical phenomena". In: *Reviews of Modern Physics* 32.2 (1960), p. 285.

[10] Adam J Bridgeman, Germán Cavigliasso, Luke R Ireland, and Joanne Rothery. "The Mayer bond order as a tool in inorganic chemistry". In: *Journal of the Chemical Society, Dalton Transactions* 14 (2001), pp. 2095–2108.

[11] Shawn T Brown, Jonathan C Rienstra-Kiracofe, and Henry F Schaefer. "A systematic application of density functional theory to some carbon-containing molecules and their anions". In: *The Journal of Physical Chemistry A* 103.20 (1999), pp. 4065–4077.

[12] MG Bulmer. *Principles of statistics, 1979*.

[13] Kieron Burke. *The ABC of DFT, http://dft.uci.edu/book/gamma/g1.pdf*. 2007. URL: http://dft.uci.edu/book/gamma/g1.pdf.

[14] Aron J. Cohen, Paula Mori-Sanchez, and Weitao Yang. "Challenges for Density Functional Theory". In: *Chemical Reviews* 112.1 (2012). PMID: 22191548, pp. 289–320. DOI: 10.1021/cr200107z. eprint: https://doi.org/10.1021/cr200107z. URL: https://doi.org/10.1021/cr200107z.

[15] C.J. Cramer. *Essentials of computational chemistry: theories and models*. Wiley, 2004. ISBN: 9780470091821. URL: https://books.google.com/books?id=1T9CAQAAIAAJ.

[16] Anita Das, Thomas Mueller, Felix Plasser, and Hans Lischka. "Polyradical Character of Triangular Non-Kekule Structures, Zethrenes, p-Quinodimethane-Linked Bisphenalenyl, and the Clar Goblet in Comparison: An Extended Multireference Study". In: *The Journal of Physical Chemistry A* 120.9 (2016). PMID: 26859789, pp. 1625–1636. DOI: 10.1021/acs.jpca.5b12393. eprint: https://doi.org/10.1021/acs.jpca.5b12393. URL: https://doi.org/10.1021/acs.jpca.5b12393.

[17] Soumyajit Das and Jishan Wu. "Open-Shell Benzenoid Polycyclic Hydrocarbons". In: Sept. 2015, pp. 1–36. ISBN: 9783527338474. DOI: 10.1002/9783527689545.ch1.

[18] Dennis A. Daugherty. "New high-spin π systems". In: *Pure & Applied Chemistry* 62.3 (1990), pp. 519–524. DOI: doi:10.1351/pac199062030519. eprint: https://doi.org/10.1351/pac199062030519. URL: https://doi.org/10.1351/pac199062030519.

[19] Jerry Ray Dias. "Concealed Coronoid Hydrocarbons with Enhanced Antiaromatic Circuit Contributions as Models for Schottky Defects in Graphenes". In: 2011.

[20] Omar ElTayeby, Dwayne John, Pragnesh Patel, and Scott Simmerman. "Comparative case study between D3 and highcharts on lustre data visualization". In: *Visualization and Data Analysis 2014*. Vol. 9017. International Society for Optics and Photonics. 2014, 90170U.

[21] Pacter G Szalay, Thomas Mueller, Gergely Gidofalvi, Hans Lischka, and Ron Shepard. "Multiconfiguration Self-Consistent Field and Multireference Configuration Interaction Methods and Applications". In: *Chemical reviews* 112 (Dec. 2011), pp. 108–81. DOI: 10.1021/cr200137a.

[22] R. Gilmore. *Alice in Quantumland*. Harcourt Trade Publishers, 1996. ISBN: 9780156004695. URL: https://books.google.com/books?id=_f_lkQEACAAJ.

[23] Eric Glendening, Clark Landis, and Frank Weinhold. *What Are "Natural Orbitals"?* URL: http://nbo6.chem.wisc.edu/webnbo_css.htm (visited on 05/26/2019).

[24] Larry Gonick and Craig Criddle. *The cartoon guide to chemistry*. 2005.

[25] D.J. Griffiths. *Introduction to Electrodynamics*. Pearson international edition. Prentice Hall, 1999. ISBN: 9780139199608. URL: https://books.google.com/books?id=x0akQgAACAAJ.

[26] Johannes Hachmann, Wim Cardoen, and Garnet Kin-Lic Chan. "Multireference correlation in long molecules with the quadratic scaling density matrix renormalization group". In: *The Journal of Chemical Physics* 125.14 (2006), p. 144101. DOI: 10.1063/1.2345196. eprint: https://doi.org/10.1063/1.2345196. URL: https://doi.org/10.1063/1.2345196.

[27] Pan Hu and Jishan Wu. "Modern zethrene chemistry". In: *Canadian Journal of Chemistry* 95.3 (2017), pp. 223–233. DOI: 10.1139/cjc-2016-0568. eprint: https://doi.org/10.1139/cjc-2016-0568. URL: https://doi.org/10.1139/cjc-2016-0568.

[28] Jingsong Huang and Miklos Kertesz. "Intermolecular Covalent π?π Bonding Interaction Indicated by Bond Distances, Energy Bands, and Magnetism in Biphenalenyl Biradicaloid Molecular Crystal". In: *Journal of the American Chemical Society* 129.6 (2007). PMID: 17284004, pp. 1634–1643. DOI: 10.1021/ja066426g. eprint: https://doi.org/10.1021/ja066426g. URL: https://doi.org/10.1021/ja066426g.

[29] Jun Inoue, Kozo Fukui, Takashi Kubo, Shigeaki Nakazawa, Kazunobu Sato, Daisuke Shiomi, Yasushi Morita, Kagetoshi Yamamoto, Takeji Takui, and Kazuhiro Nakasuji. "The First Detection of a Clar's Hydrocarbon, 2,6,10-Tri-tert-Butyltriangulene: A Ground-State Triplet of Non-Kekule Polynuclear Benzenoid Hydrocarbon". In: *Journal of the American Chemical Society* 123.50 (2001). PMID: 11741445, pp. 12702–12703. DOI: 10.1021/ja016751y. eprint: https://doi.org/10.1021/ja016751y. URL: https://doi.org/10.1021/ja016751y.

[30] Erin R. Johnson, Paula Mori-Sanchez, Aron J. Cohen, and Weitao Yang. "Delocalization errors in density functionals and implications for main-group thermochemistry". In: *The Journal of Chemical Physics* 129.20 (2008), p. 204112. DOI: 10.1063/1.3021474. eprint: https://doi.org/10.1063/1.3021474. URL: https://doi.org/10.1063/1.3021474.

[31] Georg Joos and Ira M Freeman. *Theoretical physics*. Courier Corporation, 2013.

[32] Sho Kamata, Sota Sato, Jishan Wu, and Hiroyuki Isobe. "Crystal structure of 7,15-bis(4-*tert*-butylphenyl)-1,9-dimethylheptazethrene". In: *Acta Crystallographica Section E* 73.2 (2017), pp. 99–102. DOI: 10.1107/S2056989016020247. URL: https://doi.org/10.1107/S2056989016020247.

[33] Gunnar Karlström, Roland Lindh, Per-Åke Malmqvist, Björn O Roos, Ulf Ryde, Valera Veryazov, Per-Olof Widmark, Maurizio Cossi, Bernd Schimmelpfennig, Pavel Neogrady, et al. "MOLCAS: a program package for computational chemistry". In: *Computational Materials Science* 28.2 (2003), pp. 222–239.

[34] Rollin A King, T Daniel Crawford, John F Stanton, and Henry F Schaefer. "Conformations of [10] annulene: more bad news for density functional theory and second-order perturbation theory". In: *Journal of the American Chemical Society* 121.46 (1999), pp. 10788–10793.

[35] Jing Kong and Emil Proynov. "Density Functional Model for Nondynamic and Strong Correlation". In: *Journal of Chemical Theory and Computation* 12.1 (2016). PMID: 26636190, pp. 133–143. DOI: 10.1021/acs.jctc.5b00801. eprint: https://doi.org/10.1021/acs.jctc.5b00801. URL: https://doi.org/10.1021/acs.jctc.5b0080.

[36] Akihito Konishi, Yasukazu Hirao, Masayoshi Nakano, Akihiro Shimizu, Edith Botek, Benoît Champagne, Daisuke Shiomi, Kazunobu Sato, Takeji Takui, Kouzou Matsumoto, et al. "Synthesis and characterization of teranthene: a singlet biradical polycyclic aromatic hydrocarbon having Kekulé structures". In: *Journal of the American Chemical Society* 132.32 (2010), pp. 11021–11023.

[37] Takashi Kubo, Akihiro Shimizu, Mikio Uruichi, Kyuya Yakushi, Masayoshi Nakano, Daisuke Shiomi, Kazunobu Sato, Takeji Takui, Yasushi Morita, and Kazuhiro Nakasuji. "Singlet Biradical Character of Phenalenyl-Based Kekule Hydrocarbon with Naphthoquinoid Structure". In: *Organic Letters* 9.1 (2007). PMID: 17192090, pp. 81–84. DOI: 10.1021/ol062604z. eprint: https://doi.org/10.1021/ol062604z. URL: https://doi.org/10.1021/ol062604z.

[38] Takashi Kubo, Akihiro Shimizu, Maki Sakamoto, Mikio Uruichi, Kyuya Yakushi, Masayoshi Nakano, Daisuke Shiomi, Kazunobu Sato, Takeji Takui, Yasushi Morita, et al. "Synthesis, intermolecular interaction, and semiconductive behavior of a delocalized singlet biradical hydrocarbon". In: *Angewandte Chemie International Edition* 44.40 (2005), pp. 6564–6568.

[39] H Lischka, R Shepard, I Shavitt, RM Pitzer, M Dallos, T Muller, PG Szalay, FB Brown, R Ahlrichs, HJ Boehm, et al. "Columbus: An ab initio electronic structure program, release 7.0, 2017". In: *Google Scholar There is no corresponding record for this reference* ().

[40] Hans Lischka, Ron Shepard, Russell M Pitzer, Isaiah Shavitt, Michal Dallos, Thomas Müller, Péter G Szalay, Michael Seth, Gary S Kedziora, Satoshi Yabushita, et al. "High-level multireference methods in the quantum-chemistry program system COLUMBUS: Analytic MR-CISD and MR-AQCC gradients and MR-AQCC-LRT for excited states, GUGA spin–orbit CI and parallel CI density". In: *Physical Chemistry Chemical Physics* 3.5 (2001), pp. 664–673.

[41] Hans Lischka, Ron Shepard, Franklin B Brown, and Isaiah Shavitt. "New implementation of the graphical unitary group approach for multireference direct configuration interaction calculations". In: *International Journal of Quantum Chemistry* 20.S15 (1981), pp. 91–100.

[42] John P Maier. "Electronic spectroscopy of carbon chains". In: *The Journal of Physical Chemistry A* 102.20 (1998), pp. 3462–3469.

[43] Jan ML Martin, Jamal El-Yazal, and Jean-Pierre François. "Structure and vibrational spectra of carbon clusters Cn (n= 2–10, 12, 14, 16, 18) using density functional theory including exact exchange contributions". In: *Chemical physics letters* 242.6 (1995), pp. 570–579.

[44] I Mayer. "Bond order and valence indices: A personal account". In: *Journal of computational chemistry* 28.1 (2007), pp. 204–221.

[45] Ross H. McKenzie. *Computational quantum chemistry in a nutshell*. 2017. URL: https://condensedconcepts.blogspot.com/2017/03/computational-quantum-chemistry-in.html (visited on 05/25/2019).

[46] Krešimir Molčanov and Biserka Kojić-Prodić. "Towards understanding π-stacking interactions between non-aromatic rings". In: *IUCrJ* 6.2 (2019), pp. 156–166. DOI: 10.1107/S2052252519000186. URL: https://doi.org/10.1107/S2052252519000186.

[47] Yasushi Morita, Shuichi Suzuki, Kazunobu Sato, and Takeji Takui. "Synthetic organic spin chemistry for structurally well-defined open-shell graphene fragments". In: *Nature chemistry* 3 (Mar. 2011), pp. 197–204. DOI: 10.1038/nchem.985.

[48] M.A. Morrison. *Understanding Quantum Physics: A User's Manual*. Understanding Quantum Physics: A User's Manual v. 1. Prentice Hall, 1990. ISBN: 9780137479085. URL: https://books.google.com/books?id=f6vvAAAAMAAJ.

[49] Masayoshi Nakano. "Electronic structure of open-shell singlet molecules: Diradical character viewpoint". In: *Topics in Current Chemistry* 375.2 (2017), p. 47.

[50] Masayoshi Nakano. *Excitation energies and properties of open-shell singlet molecules: applications to a new class of molecules for nonlinear optics and singlet fission*. Springer, 2014.

[51] *Natural Bond Orbital Analysis Tutorial*. URL: http://www.colby.edu/chemistry/webmo/nbotutor.html.

[52] Robert Parrish. *getLebedevSphere*. Ed. by MathWorks. URL: https://www.mathworks.com/matlabcentral/fileexchange/27097-getlebedevsphere.

[53] Niko Pavliaek, Anish Mistry, Zsolt Majzik, Nikolaj Moll, Gerhard Meyer, David Fox, and Leo Gross. "Synthesis and characterization of triangulene". In: *Nature Nanotechnology* 12 (Feb. 2017). DOI: 10.1038/nnano.2016.305.

[54] Roberto Peverati and Donald G. Truhlar. "Quest for a universal density functional: the accuracy of density functionals across a broad spectrum of databases in chemistry and physics". In: *Philosophical Transactions of the Royal Society A: Mathematical, Physical and Engineering Sciences* 372.2011 (2014), p. 20120476. DOI: 10.1098/rsta.2012.0476. eprint: https://royalsocietypublishing.org/doi/pdf/10.1098/rsta.2012.0476. URL: https://royalsocietypublishing.org/doi/abs/10.1098/rsta.2012.0476.

[55] Felix Plasser, Hasan Pašalić, Martin H Gerzabek, Florian Libisch, Rafael Reiter, Joachim Burgdörfer, Thomas Müller, Ron Shepard, and Hans Lischka. "The Multiradical Character of One-and Two-Dimensional Graphene Nanoribbons". In: *Angewandte Chemie International Edition* 52.9 (2013), pp. 2581–2584.

[56] Emil Proynov. personal communication. June 22, 2019.

[57] Emil Proynov, Fenglai Liu, and Jing Kong. "Analyzing effects of strong electron correlation within Kohn-Sham density-functional theory". In: *Phys. Rev. A* 88 (3 2013), p. 032510. DOI: 10.1103/PhysRevA.88.032510. URL: https://link.aps.org/doi/10.1103/PhysRevA.88.032510.

[58] Peter Pulay. "Convergence acceleration of iterative sequences. The case of SCF iteration". In: *Chemical Physics Letters* 73.2 (1980), pp. 393–398.

[59] *SCAN (Strongly-Constrained and Appropriately-Normed.* 2021. URL: https://templeefrc.org/scan-overview (visited on 01/31/2021).

[60] Akihiro Shimizu, Takashi Kubo, Mikio Uruichi, Kyuya Yakushi, Masayoshi Nakano, Daisuke Shiomi, Kazunobu Sato, Takeji Takui, Yasukazu Hirao, Kouzou Matsumoto, et al. "Alternating covalent bonding interactions in a one-dimensional chain of a phenalenyl-based singlet biradical molecule having Kekulé structures". In: *Journal of the American Chemical Society* 132.41 (2010), pp. 14421–14428.

[61] Akihiro Shimizu, Mikio Uruichi, Kyuya Yakushi, Hiroyuki Matsuzaki, Hiroshi Okamoto, Masayoshi Nakano, Yasukazu Hirao, Kouzou Matsumoto, Hiroyuki Kurata, and Takashi Kubo. "Resonance balance shift in stacks of delocalized singlet biradicals". In: *Angewandte Chemie* 121.30 (2009), pp. 5590–5594.

[62] Jianwei Sun. "Supplementary Material for "Strongly Constrained and Appropriately Normed Semilocal Density Fuctional". In: (2016).

[63] Jianwei Sun, John P Perdew, and Adrienn Ruzsinszky. "Semilocal density functional obeying a strongly tightened bound for exchange". In: *Proceedings of the National Academy of Sciences* 112.3 (2015), pp. 685–689.

[64] Jianwei Sun, Adrienn Ruzsinszky, and John P. Perdew. "Strongly Constrained and Appropriately Normed Semilocal Density Functional". In: *Phys. Rev. Lett.* 115 (3 2015), p. 036402. DOI: 10.1103/PhysRevLett.115.036402. URL: http://link.aps.org/doi/10.1103/PhysRevLett.115.036402.

[65] Jianwei Sun, Adrienn Ruzsinszky, and John P. Perdew. "Strongly constrained and appropriately normed semilocal density functional". In: *Physical review letters* 115.3 (2015), p. 036402.

[66] Zhe Sun, Zebing Zeng, and Jishan Wu. "Zethrenes, Extended p-Quinodimethanes, and Periacenes with a Singlet Biradical Ground State". In: *Accounts of Chemical Research* 47.8 (2014). PMID: 25068503, pp. 2582–2591. DOI: 10.1021/ar5001692. eprint: https://doi.org/10.1021/ar5001692. URL: https://doi.org/10.1021/ar5001692.

[67] Zhe Sun, Sangsu Lee, Kyu Hyung Park, Xiaojian Zhu, Wenhua Zhang, Bin Zheng, Pan Hu, Zebing Zeng, Soumyajit Das, Yuan Li, Chunyan Chi, Run-Wei Li, Kuo-Wei Huang, Jun Ding, Dongho Kim, and Jishan Wu. "Dibenzoheptazethrene Isomers with Different Biradical Characters: An Exercise of Clar's Aromatic Sextet Rule in Singlet Biradicaloids". In: *Journal of the American Chemical Society* 135.48 (2013). PMID: 24206273, pp. 18229–18236. DOI: 10.1021/ja410279j. eprint: https://doi.org/10.1021/ja410279j. URL: https://doi.org/10.1021/ja410279j.

[68] Kazuo Takatsuka, Takayuki Fueno, and Kizashi Yamaguchi. "Distribution of odd electrons in ground-state molecules". In: *Theoretica chimica acta* 48.3 (1978), pp. 175–183. ISSN: 1432-2234. DOI: 10.1007/BF00549017. URL: https://doi.org/10.1007/BF00549017.

[69] Takashi Tsuchimochi, Thomas M Henderson, Gustavo E Scuseria, and Andreas Savin. "Constrained-pairing mean-field theory. IV. Inclusion of corresponding pair constraints and connection to unrestricted Hartree–Fock theory". In: *The Journal of chemical physics* 133.13 (2010), p. 134108.

[70] Troy Van Voorhis and Martin Head-Gordon. "A geometric approach to direct minimization". In: *Molecular Physics* 100.11 (2002), pp. 1713–1721.

[71] Luc Vereecken and Joseph S. Francisco. "Theoretical studies of atmospheric reaction mechanisms in the troposphere". In: *Chem. Soc. Rev.* 41 (19 2012), pp. 6259–6293. DOI: 10.1039/C2CS35070J. URL: http://dx.doi.org/10.1039/C2CS35070J.

[72] Matthew Wang, Dwayne John, Jianguo Yu, Emil Proynov, Fenglai Liu, Benjamin G Janesko, and Jing Kong. "Performance of new density functionals of nondynamic correlation on chemical properties". In: *The Journal of chemical physics* 150.20 (2019), p. 204101.

[73] Matthew Y. Wang. "The Application of Genetic Algorithms For Density Functional Optimization and Development". PhD thesis. Middle Tennessee State University, 2019.

[74] Hans-Joachim Werner, Peter J Knowles, Gerald Knizia, Frederick R Manby, and Martin Schütz. "Molpro: a general-purpose quantum chemistry program package". In: *Wiley Interdisciplinary Reviews: Computational Molecular Science* 2.2 (2012), pp. 242–253.

[75] *What are "Natural Orbitals"?* URL: https://nbo6.chem.wisc.edu/webnbo_css.htm.

[76] Chia-Nan Yeh and Jeng-Da Chai. "Role of Kekulé and non-Kekulé structures in the radical character of alternant polycyclic aromatic hydrocarbons: a TAO-DFT study". In: *Scientific reports* 6 (2016), p. 30562.

[77] M. Zander. "Polycyclic Hydrocarbons". In: *Angewandte Chemie* 77.19 (1965), pp. 875–876. DOI: 10.1002/ange.19650771941. eprint: https://onlinelibrary.wiley.com/doi/pdf/10.1002/ange.19650771941. URL: https://onlinelibrary.wiley.com/doi/abs/10.1002/ange.19650771941.

[78] M. Zander. "Polycyclic Hydrocarbons. Band II. Von E. Clar. Academic Press, London-New York; Springer-Verlag, Berlin-Gattingen-Heidelberg 1964. 1. Aufl., LVIII, 487 S., 153 Abb., geb. DM 78.40." In: *Angewandte Chemie* 77.19 (1965), pp. 876–876. DOI: 10.1002/ange.19650771942. eprint: https://onlinelibrary.wiley.com/doi/pdf/10.1002/ange.19650771942. URL: https://onlinelibrary.wiley.com/doi/abs/10.1002/ange.19650771942.

[79] Andrew Zangwill. "density functional theory". In: *Physics today* 68.7 (2015), p. 34.

[80] Yan Zhao and Donald G Truhlar. "The M06 suite of density functionals for main group thermochemistry, thermochemical kinetics, noncovalent interactions, excited states, and transition elements: two new functionals and systematic testing of four M06-class functionals and 12 other functionals". In: *Theoretical Chemistry Accounts* 120.1-3 (2008), pp. 215–241.

10 APPENDIX

```
      SUBROUTINE scan_modified(INFOR,NDEN,NG,NA,NB,THRESH,
     $RhoA,RhoB,DRA,DRB,TauA,TauB,F,D1F)
c     ****************************************************************
c     *                                                              *
c     *  Strongly Constrained and Appropriately Normed               *
c     *  (SCAN) Semilocal Density Functional Calculaion              *
c     *  SCAN functional calculation of functional                   *
c     *                                                              *
c     *   input:                                                     *
c     *   INFOR:       information array about variable position     *
c     *   NDEN:        number of density(close shell: 1, open shell: 2) *
c     *   NG:          number grid points (NG) keep                  *
c     *   THRESH:      threshold to determine the small rho etc.(keep) *
c     *   RhoA,RhoB:   spin density ( n in SCAN paper ) (keep)       *
```

```
c     *   DRA,DRB:     gradient of spin density (grad(n) in SCAN paper) *
c     *   TauA,TauB:   kinetic density (keep)                           *
c     *                                                                 *
c     *   output:                                                       *
c     *   F:          functional value  (Total Energy) = Exchange       *
c     *               + Correlation Energy                              *
c     *   D1F:        functional derivatives                            *
c     *                                                                 *
c     *   s:          the dimensionless density gradient                *
c     *   n:          the spin charge density 2*RA                      *
c     *   alpha1:     the dimensionaless variable as a function of Tau  *
c     *   TauW:       the single-orbital limit of Tau Weizsaecker       *
c     *               kinetic energy density                            *
c     *   Tau_unif:   the uniform-density limit of Tau                  *
c     *                                                                 *
c     *   Author: Dwayne John                                           *
c     *                                                                 *
c     *******************************************************************
      IMPLICIT NONE
      INTEGER NDEN,NG,I,J,method
      INTEGER NA,NB
      INTEGER INFOR(*)
      REAL*8 PI
      REAL*8 C
      REAL*8 THRESH
      REAL*8 RhoA(NG),RhoB(NG),DRA(NG,3),DRB(NG,3)
      REAL*8 TauA(NG),TauB(NG)
      REAL*8 F(NG),D1F(NG,*)
      REAL*8 RA,RB
      REAL*8 GAA,GBB,GAB !Gradient of n
      REAL*8 GB
      REAL*8 TA,TB
      REAL*8 UA,UB
#include "fderiv1.inc"

      ! constant
      INTEGER D1VARS(N_FUNC_DERIV_1)
      REAL*8 ZERO
      REAL*8 ONE,TWO,THREE,FOUR,FIVE,EIGHT,NINE
      REAL*8 F12,F14,F13,F53,F23,F112

          real(8), dimension(NG) :: Ex
          real(8) :: c1x,c2x,dx,k1,a1,h0x,mu_ak,b2,b1,b3,b4
          real(8) :: alpha1,a
          real(8) :: x,x1,x2,h1x,gx,fx,fx1,fx2,dfx
          real(8) :: Fex,exc, ex_unif
          real(8) :: grad_s,n,grad_n,s,TauW,Tau_unif,Tau
          integer :: row_alpha,col_alpha,m
          integer :: theta1,theta2

          fex = 0.d0
          fx = 0.d0
```

```
67            fx1 = 0.d0
68            fx2 = 0.d0
69          ! Parameters for fx
70            c1x = 0.667
71            c2x = 0.8
72            dx = 1.24
73            k1 = 0.065
74            a1 = 4.9479
75            h0x = 1.174
76            mu_ak = 10.0/81.0
77            b2 = SQRT(5913.0/405000.0)
78            b1 = (511.0/13500.0)/(2.0*b2)
79            b3 = 0.5
80            b4 = (mu_ak**2.0d0)/k1 - (1606.0/18225.0) - (b1**2.0d0);
81
82          ! constants
83          PI    = 4.D0*DATAN(1.D0)
84          ! firstly initilize variable position information
85          CALL INIT_FUNC_DERIV_1(INFOR,D1VARS)
86
87          ! loop over the number of grid points
88          DO I = 1,NG
89              write(6,*)"      "
90              write(6,*)"_____________________"
91              write(6,*)"for grid: ", i
92
93              ! variables
94              RA  = RhoA(i)
95              write(6,*)"RA = ", RA
96              RB  = RhoB(i)
97              write(6,*)"RB = ", RB
98              GAA = DRA(i,1)*DRA(i,1) + DRA(i,2)*DRA(i,2)
99         &+ DRA(i,3)*DRA(i,3)
100             write(6,*)"GAA = ",GAA
101             GAB = DRA(i,1)*DRB(i,1) + DRA(i,2)*DRB(i,2)
102        &+ DRA(i,3)*DRB(i,3)
103             write(6,*)"GAB = ",GAB
104             GBB = DRB(i,1)*DRB(i,1) + DRB(i,2)*DRB(i,2)
105        &+ DRB(i,3)*DRB(i,3)
106             write(6,*)"GBB = ",GBB
107             TA  = TauA(i)
108             write(6,*)"TA = ",TA
109             TB  = TauB(i)
110             write(6,*)"TB = ",TB
111
112              n = 2.0d0*RB
113              write(6,*)"n = ",n
114              grad_n = sqrt(GAA+GBB+2*GAB)
115              write(6,*)"grad_n = ",grad_n
116              s = abs(grad_n)/(2.0d0*(3.0d0*(PI**2.0d0))**(1.0d0/3.0d0)
117         $*n**(4.0d0/3.0d0))
118              write(6,*)"s = ",s
```

```
119           TauW = (grad_n**2.0d0)/(8.0*n)
120           write(6,*)"TauW = ",TauW
121           Tau_unif = (3.0/10.0)*(3.0*(PI**2.0d0))**(2.0d0/3.0d0)
122          $*(n**(5.0d0/3.0d0))
123           write(6,*)"Tau_unif = ",Tau_unif
124           Tau = TB !Perdew uses Tau with a 1/2 factor?
125           write(6,*)"Tau = ",Tau
126           alpha1 = (Tau - TauW)/Tau_unif
127           write(6,*)"Alpha1 = ",alpha1
128
129           x = mu_ak*(s**2.0d0) * ( 1.d0 + ( (b4*(s**2.d0))/mu_ak )
130          $* exp((-abs(b4)*(s**2.d0))/mu_ak) ) + (b1*(s**2.d0) + b2
131          $* (1.d0 - alpha1)*exp(-b3*(1.d0 - alpha1)**2.d0) )**2.d0
132           write(6,*)"x = ",x
133
134           x1 = 1.d0 - alpha1
135           write(6,*)"x1 = ",x1
136           x2 = alpha1 - 1.d0
137           write(6,*)"x2 = ",x2
138
139           !Basic Heaviside step function code implementation
140           if(x1 < 0.d0) then
141             theta1 = 0.d0
142             theta2 = 1.d0
143           else if(x1 > 0.d0) then
144             theta1 = 1.d0
145             theta2 = 0.d0
146           else
147             theta1 = 0.5d0
148             theta2 = 0.5d0
149           end if
150
151         write(6,*)"theta1 = ",theta1
152         write(6,*)"theta2 = ",theta2
153
154         h1x = 1.d0 + k1 - ( k1 / (1.d0 + (x/k1) ) )
155         write(6,*)"The value of h1x = ",h1x
156
157         !Note the author has a positive (1.d0/2.d0) in his code
158         gx = 1.d0 - exp(-a1*(s**(-1.0d0/2.0d0)))
159         write(6,*)"The value of gx = ",gx
160
161         fx1 = exp( (-c1x*alpha1)/(1.d0-alpha1 ) )*theta1
162         if(fx1 /= fx1) then !Handles NaN issues
163            fx1 = 0.d0
164         end if
165         write(6,*),"The value of fx1 = ",fx1
166
167         fx2 = -dx*exp( c2x/(1.d0-alpha1) )*theta2
168         if(fx2 /= fx2) then !Handles NaN issues
169            fx2 = 0.d0
170         end if
```

```
171         write(6,*),"The value of fx2 = ",fx2
172
173         fx = fx1 + fx2
174         write(6,*),"The value of fx = ",fx
175
176         Fex = (h1x + fx * (h0x - h1x) )*gx
177         write(6,*),"Fex= ",Fex
178
179         ex_unif = -(3.0d0/(4.0d0*PI))*(3.0d0*(PI**2.d0)*n)**(1.d0/3.d0)
180         write(6,*),"ex_unif = ",ex_unif
181         exc = ex_unif * n
182         write(6,*),"exc = ",exc
183
184         !Numerical Integration sum
185         F(i) = F(i) + exc*Fex
186         write(6,*),"F(i) + exc*Fex = ",F(i)
187         write(6,*),"F(i) = ",F(i)
188
189         END DO
190         RETURN
191         END
```

scan_modified.f